FINAL REPORT

Title: The Role of Composition and Particle Size on the Toxicity of Wildfire Emissions

JFSP PROJECT ID: 14-1-04-16

December 2018

M. Ian Gilmour
EPHD, NHEERL, U.S. Environmental Protection Agency

Yong Ho Kim
National Research Council

Mark Higuchi
EPHD, NHEERL, U.S. Environmental Protection Agency

Michael Hays
AEMD, NRMRL, U.S. Environmental Protection Agency

Aimen Farraj
EPHD, NHEERL, U.S. Environmental Protection Agency

David DeMarini
ISTD, NHEERL, U.S. Environmental Protection Agency

FIRESCIENCE.GOV
Research Supporting Sound Decisions






Table of Contents

List of Tables

List of Figures

List of Abbreviations/Acronyms

PM – Particulate matter
EF – Emission factor
CO – Carbon monoxide
CO_2 – Carbon dioxide
PID – Proportional-integral-derivative
NO – Nitrogen monoxide
NO_2 – Nitrogen dioxide
GSD – Geometric standard deviation
MMD – Mass median diameter
MCE – Modified combustion efficiency
MJ_{th} – Megajoulethermal
OC – Organic carbon
EC – Elemental carbon
PAH – Polycyclic aromatic hydrocarbon
VOC – Volatile organic compounds
LPS – Lipopolysaccharide
COHb – Carboxyl hemoglobin
MV – Minute ventilation
TV – Tidal volume
F – Breathing frequency
RT – Relaxation time
Ti – Inspiratory time
Te – Expiratory time
PIF – Peak inspiratory
PEF – Peak expiratory
Penh – Enhanced pause
BALF – Bronchoalveolar lavage fluid
LDH – Lactate dehydrogenase
GGT – Gamma-glutamyl transferase
NAG – N-acetyl-beta-glucoaminidase
TNF-α – Tumor necrosis factor-α
IL-6 – Interleukin-6
MIP-2 – Macrophage inhibitory protein-2
MPPD – Multiple-path particle dosimetry
DCM – Dichloromethane
EOM – Extractable organic material
DMSO – Dimethyl sulfoxide
ANOVA – Analysis of variance
SEM – Standard error of the mean
HF – High fat
FA – Filtered air
IVCT – Isovolumic contraction time
IVRT – Isovolumic relaxation time

AET – Aortic ejection time
MIA – Microalbumin
AGP – Alpha-1 acid glycoprotein
PBS – Phosphate-buffered saline

Keywords

Wildland fires, Particulate matter, Emission factor, Smoldering, Flaming, Biomass smoke, Biomass fuel, Cryotrap system, Quartz tube furnace, Oropharyngeal aspiration, Inhalation, Lung toxicity, Cardiac toxicity, Mutagenicity, Health effect

Acknowledgements

The authors would like to thank Carey Copeland, Lisa Copeland, Wanda Williams, Rachel Grindstaff, Debora Andrews, and Judy Richards for technical assistance in toxicological analyses; John McGee and Dr. Kasey Kovalcik for technical assistance in PM chemical analyses; Brandi Martin and Drs. Mehdi Hazari and Leslie Thompson for cardiac toxicity assessments. Drs. Stephen Gavett and Marie McGee for pulmonary function testing, and Dr. Shawn Urbanski (Missoula Fire Sciences Laboratory) for kindly providing biomass samples.

The research described in this manuscript has been reviewed by the National Health and Environmental Effects Research Laboratory, U.S. Environmental Protection Agency, and approved for publication. Approval does not signify that contents necessarily reflect the views and policies of the Agency, nor does the mention of trade names or commercial products constitute endorsement or recommendation for use. The authors declare that they have no competing financial interests.

Abstract

Acute and chronic exposure to wildfire smoke can cause numerous documented cardiopulmonary effects, although determining the casual components within the thousands of different chemicals found in both the particle and gas phases remains a toxicological challenge. Specifically, little work has been done to evaluate and predict toxicity of wildfire smoke including 1) how toxic is wildfire smoke compared to other pollutants, 2) which components in wildfire smoke are responsible for adverse health outcomes, and 3) whether the toxicity of wildfire smoke is governed by fuel type and combustion conditions. In this research project, we evaluated lung toxicity, cardiac toxicity and mutagenicity of particulate matter (PM) from flaming and smoldering phases of five biomass fuels (oak, peat, pine needles, pine, and eucalyptus). Biomass smoke condensates were collected from a quartz-tube furnace generation system coupled to a multistage cryotrap. The samples were chemically analyzed and assessed for lung toxicity by oropharyngeal aspiration in mice (non-inhalation exposure study) and mutagenicity in Salmonella. Biomass smoke PM was also directly delivered to mice or rats for inhalation exposure testing for lung and cardiac toxicity tests. Results from the aspiration exposure study showed that, on an equal mass exposure basis, the eucalyptus (flaming) and peat (flaming) smoke PM induced significant lung toxicity potencies (toxicity per mass of PM) compared to smoldering smoke PM, while high levels of mutagenicity potencies were observed for the pine (flaming) and peat (flaming) smoke compared to smoldering smoke. When effects were adjusted for emission factor (which reflects exposure based on mass of fuel consumed), pine (smoldering) and pine needles (smoldering) smoke PM had the highest mutagenicity emission factors (toxicity per thermal energy of fuel combustion) and these were approximately 5, 10, and 30 times greater than those reported for open burning of agricultural plastics, wood burning cookstoves and municipal waste combustors, respectively. The inhalation exposure study also demonstrated that the peat (flaming and smoldering) and eucalyptus (smoldering) smoke elicited significant inflammation in mouse lungs. No responses were seen in aspiration and inhalation studies for emissions from oak smoke. Peat (smoldering) smoke also sensitized rats to post-high fat meal cardiometabolic responses, including significantly increased cardiac isovolumic relaxation time and proinflammatory blood monocytes. Overall, the lung toxicity potencies agreed well between aspiration and inhalation studies with the results showing that although flaming smoke contains much less PM mass than smoldering smoke, it was, on a mass basis, more toxic and mutagenic than smoldering smoke, and that fuel type is also a controlling factor. Knowledge of the differential toxicity of biomass emissions will contribute to more accurate hazard assessment of biomass smoke exposures.

Objectives

The overall goals of this research were to 1) investigate the relative cardiopulmonary toxicity and mutagenicity of biomass smoke emissions from smoldering and flaming combustion conditions of different biomass fuels, 2) provide a ranking of the adverse effects and compare to other ambient air pollutant samples, and 3) determine key chemical component(s) in the biomass smoke responsible for the adverse toxic effects. To address these questions, we hypothesized that 1) coarse particles from combustion emissions primarily affect the pulmonary system, whereas fine/ultrafine particles have an effect on the cardiovascular system, 2) cardiac effects of fine/ultrafine particles in biomass smoke are driven by semi-volatile organics that vary depending on the types of fuel and combustion conditions, 3) fine/ultrafine particles are more mutagenic than coarse particles, and 4) peat smoke is more toxic than oak or pine smoke and the adverse effect is related to levels of endotoxin. As the project commenced it was clear that the smoke generated

from the laboratory system comprised only fine/ultrafine particles with no appreciable coarse particles being measured. In addition, since endotoxin has been most associated with coarse particles in the ambient environment, and only low levels of endotoxin were detected in the biomass smoke generated here we re-focused the research on assessing the role of organic chemical components instead of endotoxin on the relative toxicity of each biomass smoke particle.

Although we originally proposed a single oropharyngeal aspiration approach (i.e., non-inhalation exposure) to deliver biomass smoke particles in the mouse lungs for the lung toxicity test, the exposure method is limited in the extent to which it mimics real-world inhalation conditions. Thus, we also developed a whole-body inhalation exposure method to study physiologically relevant exposures and compared toxicity outcomes with the aspiration exposure. We also assessed cardiocascular function in some instances in rats fed a high fat diet. With these extended study objectives we were able to 1) address whether toxicity of smoke emissions from wildfires varies depending on the types of fuel, combustion conditions and the resultant particle chemistry, 2) expand the knowledge of the relative toxicity of different smoke emissions, 3) provide a data base that could lend itself to a systematic comparison with other ambient air pollutants, and 4) calculate relative toxicity potency values to help regulators decide whether to adhere to the national ambient air quality standards.

Background

Each year tens of millions of people globally experience destructive wildland fires and subsequent health impacts from smoke exposure (UNEP 1999). Trends for warmer and drier conditions are expected to result in greater frequency, size, and intensity of wildfires in many parts of the world (Abatzoglou and Williams 2016; Westerling et al. 2006). Besides the direct threat of fire itself, wildland fire smoke poses significant threats to firefighter and public health, leading to an increased risk of serious symptoms (e.g., pneumonia, emphysema, and heart failure) (Liu et al. 2015; Youssouf et al. 2014). It is also well recognized that exposures to wildland fire smoke may worsen symptoms for people with pre-existing health conditions (e.g., asthma and cardiovascular disease) (Cascio 2018). Recent reviews cite numerous studies that have reported associations between wildland fires and health outcomes, including respiratory infections, asthma, cardiovascular diseases, and mortality (Liu et al. 2015; Reid et al. 2016). More specifically it was estimated in one report that worldwide exposures to fine fraction (<2.5 μm) particulate matter (PM2.5) from wildland fires during 1997 – 2006 were associated with approximately 340,000 deaths per year, with larger numbers of deaths during years with dryer conditions and more fires (Johnston et al. 2012).

Despite the public health threat from an increased exposure to wildland fire smoke, studies examining the specific role of smoke components on disease incidence or severity following exposure are lacking. Specifically, it is important to determine whether the chemical composition of the emissions vary with the types of fuel burned and combustion conditions (flaming versus smoldering), and how these variables affect the potential health effects of the resulting emissions. Of the myriad components in wildland fire smoke, primary and secondarily formed PM are major factors of concern because they can remain in the air for days or weeks and can be transported over long distances (Reisen et al. 2015). The spatio-temporal variability of PM, including smoldering versus flaming emissions, can complicate the characterization of health risks of wildland fire smoke exposure to firefighters and the general public (Adetona et al. 2016).

Several studies have compared the chemical composition of PM from wildland fires or laboratory combustions of different fuel types under different burning conditions (Burling et al.

2010; Gilman et al. 2015; McMeeking et al. 2009; Reid et al. 2005); however, less work has integrated these findings with toxicological effects of the emissions. Since biomass smoke is strongly influenced by the dynamic and relatively unpredictable nature of its combustion it is challenging to maintain stable conditions and concentrations for toxicity testing. Moreover, due to considerable variability in study design and combustion conditions within and among laboratories, it is difficult to compare toxicological findings across reported studies.

To address these issues, we generated biomass smoke during flaming or smoldering phases of combustion from five different fuel types using a quartz-tube furnace that produces stable, reproducible smoke over a one hour period. The system was coupled to a multi-stage cryo-trap system that efficiently collected PM condensates for lung toxicity and mutagenicity tests. We further developed an automated smoke concentration control system to more precisely maintain biomass smoke concentrations to generate emissions from different fuels with reproducible physico-chemical characteristics. These emissions were also directly used for lung and cardiac toxicity tests. To our knowledge, this represents the first fully-automated furnace system for biomass smoke production that can be used to provide accurate toxicological profiles from well-defined biomass smoke emissions. We burned red oak, peat, pine needles, pine, and eucalyptus under flaming and smoldering phases to represent contrasting fuel types. These fuel types were selected as surrogates for major forest types across the United States (U.S.).

Materials and Methods

Biomass Combustion and Exposure System

Biomass Fuel Types

In consultation with the JFSP science advisory committee we selected 5 different biomass fuels for study: northern red oak, pocosin peat, ponderosa pine needles, lodgepole pine, and eucalyptus. Red oak was used to represent eastern and central wildland fires in the U.S. and was obtained from the Air and Energy Management Division at the U.S. Environmental Protection Agency (EPA). Peat was used to represent peatland/coastal wildfires, which are found mostly in the midwestern and southeastern U.S. Peat was collected from the coastal oligotrophic plain of eastern North Carolina (Alligator River National Wildlife Refuge) using a "Russian Peat borer tool" (De Vleeschouwer et al. 2010), or was purchased as "irish peat" from commercial suppliers (Glynn Bros, Boston, MA). Ponderosa pine needles and lodgepole pine were used to represent western wildland fires in the U.S. and were provided by the U.S. Forest Service Missoula Fire Sciences Laboratory. Eucalyptus (purchased commercially from Woodworkers Source, AZ) was used to represent chaparral (i.e., fire-prone) biome-type wildland fires, which are found in most of the southern part of coastal California in the U.S. as well as other continents (e.g., the west coast of South America and the southwestern Australia) (Kellison et al. 2013). The red oak, pine, and eucalyptus samples were cut into approximately 2-cm long wood chips to facilitate uniform combustion conditions. The peat sample was crumbled into a loose agglomerate, whereas the pine needles were burned without further processing. All biomass fuels were stored in a temperature- and humidity-controlled room (23°C and 39% relative humidity, RH) until used.

*Tube Furnace and Cryotrap System (**for Lung Toxicity and Mutagenicity Study**)*

Biomass combustion was conducted in a quartz-tube furnace (Klimisch et al. 1980; Werley et al. 2009) under both smoldering and flaming phases (Figure 1). This system consisted of a quartz tube (1-m long and 3.8-cm diameter) and a ring furnace (11.4-cm long). The furnace surrounding the quartz tube was mounted on a linear actuator driven with a combination travel speed controller

that was set to maintain a speed of 1 cm/min as it traversed along the length of the quartz tube. The biomass fuel (15 g) was placed uniformly inside the length of the quartz tube, and the temperature was adjusted to achieve steady-state smoldering (~500°C) and flaming (~640°C) combustion conditions. The furnace system was able to sustain stable flaming or smoldering phases consistently for 60 min. The primary air flow (air through the quartz tube) was approximately 2 L/min.

We collected the smoke using a multi-stage cryotrap system (Figure 1). This system was employed for two principal reasons: 1) to collect volatile and semi-volatile components, which typically pass through filters, and 2) to collect particles, which are difficult to extract from filter matrixes. Half of the outlet biomass smoke flow (approximately 1 L/min) from the tube furnace was drawn into the cryotrap system consisting of three sequential impingers maintained at -10°C, -50°C, and -70°C. PM and condensable gas-phase semi-volatiles in the biomass smoke (termed 'smoke condensate' henceforth) were captured by cryogenic trapping in the impingers. Each impinger was packed with mixed-size glass beads (1- and 0.4-cm diameter) to provide a large surface area for collection of the smoke. The other half of the biomass smoke flow (approximately 1 L/min) was diluted with secondary air flow (15 L/min) and then analyzed continuously for carbon dioxide (CO_2) and carbon monoxide (CO) using a non-dispersive infrared analyzer (Model: 602 CO/CO2; CAI Inc., Orange, CA).

We also collected PM on glass-fiber filters installed in both the exhaust line of the tube furnace and the cryotrap system exhaust during the combustion (60 min) and determined mean PM concentrations gravimetrically by weighing the filter before and after PM collection. Particle-size distributions (in the range of 32 nm to 10.57 µm) were monitored in real-time by an electrical low-pressure impactor (ELPI; Model: 97 2E; Dekati Ltd, Tampere, Finland). Number-based size distribution data were converted into the surface-area weighted distributions using the ELPIvi software (Schmid and Stoeger 2016). Flow rates of the biomass smoke were precisely controlled by a vacuum controller (Model: XC-40; Apex Instruments Inc., Fuquay-Varina, NC) located at the end of each exhaust line. A pressure gauge (Magnehelic, Dwyer Instruments Inc., Michigan City, IN) was placed in the outlet of the tube furnace to ensure a constant pressure drop throughout each burn.

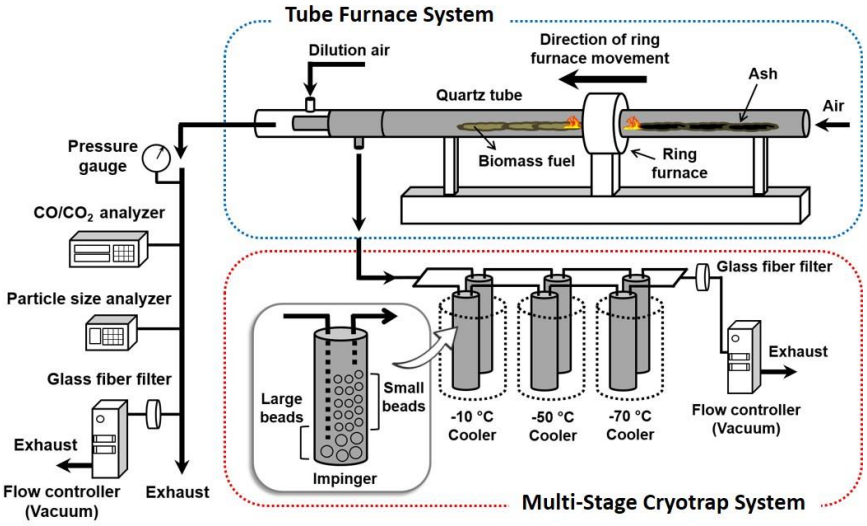

Figure 1. Diagram of the biomass combustion and smoke collection system.

*Inhalation Exposure System (**for Lung Toxicity Study**)*

We modified the tube furnace system to precisely control both the combustion phases as well as the biomass smoke concentrations (i.e., PM and carbon monoxide). An automated smoke dosage control system incorporating a proportional-integral-derivative (PID) feedback loop coupled with a mass flow controller (Mass-Flo, MKS Instrument, Inc., Andover, MA) was designed and integrated into the quartz-tube furnace system to maintain constant smoke exposure. A schematic diagram of the automatic smoke dosage control system with an inhalation exposure chamber is shown in Figure 2. Biomass smoke (2 L/min) generated from the tube furnace system under smoldering or flaming conditions was diluted with air (nominally 2.5 and 40 L/min for 1st and 2nd dilution air, respectively) and then delivered to an inhalation chamber (64 port stainless steel chamber, Laboratory Products Inc., Seaford, DE). The smoke PM concentration was continuously monitored and used to adjust the PID feedback control loop linked to an exhaust flow control valve in the smoke inlet line. System flow adjustments were continuously made in response to changes in PM concentration in the exposure chamber, thus maintaining the PM concentrations within <10% of the target set value. The diluted biomass smoke through each port on the exposure chamber was maintained at a flow rate of approximately 1 L/min. The chamber temperature and relative humidity were maintained at 22°C and 40%, respectively. Carbon dioxide (CO_2) and carbon monoxide (CO) levels were monitored using a non-dispersive infrared analyzer (Model: 602 CO/CO2; CAI Inc., Orange, CA) and nitrogen oxides (NO, NO2, and NOx) levels were measured with a chemiluminescent analyzer (Model: 42i NO/NO2/NOx; Thermo Scientific, Franklin, MA). PM was collected on a glass-fiber filter installed in the exhaust line of the inhalation chamber to determine mean PM concentrations gravimetrically by weighing the filter before and after inhalation exposure. Particle-size distributions (in the range of 10 nm to 10 μm) were monitored using a scanning mobility particle sizer (NanoScan SMPS, Model:3910; TSI Inc., Shoreview, MN) combined with an optical particle sizer (OPS, Model: 3330; TSI Inc.). Real-time measurements of biomass smoke properties and engineering parameters (e.g., temperatures, relative humidities, static pressures, and flow rates) were continuously monitored, recorded, and displayed using data acquisition software (Dasylab version 13.0, National Instruments, Austin, TX).

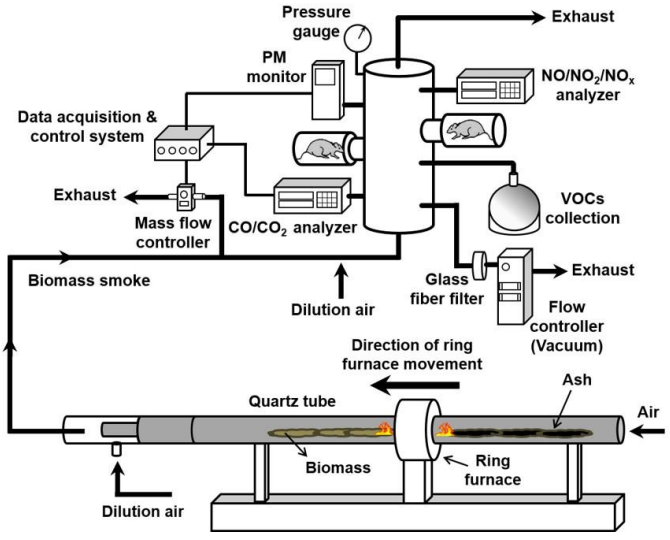

Figure 2. Diagram of the automated combustion control system for inhalation exposure to biomass smoke

*Inhalation Exposure System (**for Lung and Cardiac Toxicity Study**)*

We generated smoldering peat smoke using an automated tube furnace system described above. A schematic diagram of the automatic smoke dosage control system with an inhalation exposure chamber for cardiopulmonary toxicity test is shown in Figure 3. Biomass smoke (2 L/min) generated from the tube furnace system was diluted with air (~3 and ~60 L/min for 1st and 2nd dilution air, respectively) and then delivered to a whole body inhalation chamber (0.3 m^3 Hinners style stainless steel and glass exposure chamber) (Hinners et al., 1968). The smoke concentration was continuously monitored and adjusted by the PID feedback control loop linked to a continuous PM monitor in the chamber to an exhaust flow control valve in the smoke inlet line. We conducted PM sampling through ports on the inhalation chamber during combustion for analysis of carbon species. Additional details of the inhalation exposure system are provided in our previous report (Martin et al. 2018).

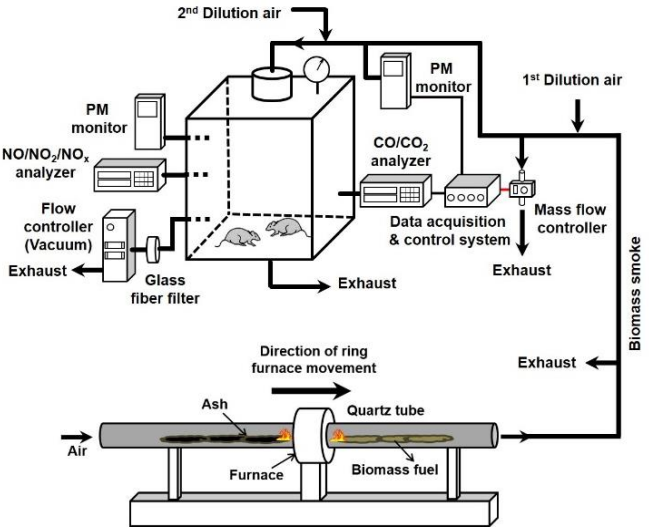

Figure 3. Diagram of the automated combustion control system for inhalation exposure to biomass smoke

Biomass Smoke Characterization

Characteristics of Biomass Smoke

Concentrations of CO_2, CO, and PM were used to continuously characterize the biomass smoke emissions. Flaming and smoldering combustion phases are typically characterized by modified combustion efficiency (MCE), which is defined as MCE (%) = (ΔCO_2 / (ΔCO_2 + ΔCO)) × 100, where ΔCO_2 and ΔCO are the excess concentrations of CO_2 and CO (Ward and Radke 1993). We considered combustion to be flaming when the MCE was >95% and smoldering when MCE was 65 – 85%, as suggested by (Urbanski 2014).

Smoke properties are also described using emission factors (EFs). In order to validate EFs estimated from the tube furnace, EFs for CO, CO_2, and PM were compared with the published EFs from various fuel combustion conditions (in-ground versus above-ground biomass fuels). We also expressed EFs per megajoulethermal (MJ_{th}) by using the heat energy (MJ_{th}/kg) of each fuel burned, which was 21.70 for the red oak (Peter 1979), 23.00 for the peat (Morvay and Gvozdenac 2008), 11.96 for the pine needles (de Muñiz et al. 2014), 20.00 for the pine (Nielson et al. 1985), and 19.25 for the eucalyptus (de Muñiz et al. 2014).

Biomass Smoke Condensate Analysis

Following the combustion tests, we extracted smoke condensate from the cryogenically cooled impingers and loose beads by washing them with acetone. We then pooled the smoke condensate suspension and concentrated it with a rotary evaporator (Model: Rotavapor R-200; Buchi, New Castle, DE). The smoke condensate was then dried under nitrogen gas to obtain predominantly solid PM (termed 'dried smoke condensate' or 'PM' henceforth) which underwent subsequent analyses.

For carbon species analysis, the aliquot of the smoke condensate suspension was pipetted onto pre-baked quartz filter punches, dried, and analyzed for organic carbon (OC) and elemental carbon (EC) with a carbon analyzer (Model: 107A; Sunset Laboratory Inc., Tigard, OR). The OC fraction was further analyzed for polar (methoxyphenols and levoglucosan) and non-polar (polycyclic aromatic hydrocarbons (PAHs) and n-alkanes) organic compounds with a thermal desorption unit (TD; Model: TDSA2/TDS, Gerstel Inc., Baltimore, MD) coupled to a gas chromatograph-mass spectrometer (GC-MS; Models: 6890-5973, Agilent Technologies Inc., Santa Clara, CA). For inorganic elemental analysis, the dried smoke condensate was digested in aqua regia and then assayed for target inorganic elements by high-resolution-magnetic sector field inductively coupled plasma mass spectrometry (HR-ICP-MS; Model: Element 2; Thermo Scientific). For ion analysis, the dried smoke condensate was diluted in ultrapure water, sonicated, and analyzed for ionic species using a dual ion chromatography system (Model: ICS2000; Dionex, Sunnyvale, CA). The smoke condensate suspension (in acetone) was solvent-exchanged into saline at a final concentration of 2 mg PM/mL and then further analyzed for pH and endotoxin levels. The pH value was measured with a calibrated pH meter (Model: 440; Corning, Woburn, MA). For the endotoxin measurement, the dried smoke condensate suspension (in saline) was vortexed and sonicated to ensure homogeneity, and then diluted in endotoxin-free water at a concentration of 1 mg/mL. Endotoxin measurements were performed using the Limulus amebocyte lysate assay (Model: QCL-1000; Lonza, Walkersville, MD) as per the manufacturer's protocol. Aliquots of the dried smoke condensate suspensions (in saline) were stored at −80°C until toxicity testing. Additional details of the smoke condensate analysis are provided in our previous report (Kim et al. 2018).

Volatile Organic Carbon Analysis

Volatile organic compounds (VOCs) and PM samples were obtained from ports on the inhalation chamber for further speciation and analysis. VOCs in the biomass smoke and filtered air (control) were sampled using SUMMA canisters and carbonyls were sampled with 2,4-dinitrophenylhydrazine (DNPH)-coated silica cartridges (PN 505323, Sigma-Aldrich Co., St. Louis, MO). The sampling flow rates through the evacuated canister (filled to approximately 0.7 atm) were controlled using a critical orifice at a flow rate of approximately 70 mL/min. Cartridge sampling flow rates were controlled with a SKC Aircheck Sampling Pump (Model: 224-PCXR8, SKC Inc., Eighty Four, PA) with flow rates in the range of 0.5 – 0.7 L/min.

Lung Toxicity of Biomass Smoke Condensates in Mice and Mutagenicity Testing

Experimental Animals

Adult pathogen-free female CD-1 mice and Balb/cJ mice (approximately 20 g body weight) were purchased from Charles River Breeding Laboratories (Raleigh, NC) and used in the oropharyngeal aspiration (non-inhalation exposure) study and the inhalation study, respectively. Mice were housed in polycarbonate cages with hardwood chip bedding at the U.S. Environmental

Protection Agency (EPA) Animal Care Facility, which is accredited by the Association for Assessment and Accreditation of Laboratory Animal Care and were maintained on a 12-h light to dark cycle at 22.3 ± 1.1°C temperature and 50 ± 10% humidity. Mice were given access to rodent chow and water ad libitum and were acclimated for at least 10 days before the study began. The studies were conducted after approval by the EPA Institutional Animal Care and Use Committee.

Oropharyngeal Aspiration Exposure to Biomass Smoke PM

We solvent-exchanged the smoke condensate suspension in acetone into saline to a final PM concentration of 2 mg/mL and then administered it into the lungs of CD-1 mice at 100 µg in 50 µL by oropharyngeal aspiration. We chose a single PM dose of 100 µg because 1) this dose represents a peak 24 h exposure for a wildfire event and 2) this dose (equivalent to 154 ng/cm^2 in mouse lungs) appeared to be relevant to the inhaled wildfire PM concentrations in the human lungs. Additional details of the selection of PM dose are provided in our previous report (Kim et al. 2018). We instilled additional mice with 2 µg of lipopolysaccharide in 50 µL saline (LPS) as a positive control to demonstrate maximal responsiveness to this well characterized inflammatory agent. We also instilled additional mice with 50 µL saline alone as a negative control.

Inhalation Exposure to Biomass Smoke

The inhalation exposures were conducted with mice being individually housed in larger rat restraint tubes that were inserted into ports of a "nose and mouth only" exposure chamber, allowing free movement (Wong 2007). Mice were exposed to the biomass smoke (smoldering and flaming) for 1 h per day for 2 days. Because CO in biomass smoke can elicit its own health impacts in terms of altering respiratory rate, vascular function and other endpoints (Canova et al. 2010; Otterbein et al. 2000; Rose et al. 2017), we elected to hold the exposures to similar concentrations of CO to compare how different PM levels might affect the lung responses. Preliminary testing during combustion runs showed that the highest PM concentrations achievable from flaming combustion with no dilution approximated 4 mg/m^3, with CO levels between 50 and 100 ppm. When smoldering conditions were used, the similar range of CO obtained through a PID feedback dilution mechanism yielded PM levels of approximately 40 mg/m^3. Thus, biomass smoke concentrations in the inhalation chamber were set at 40 and 4 mg/m^3 of PM for smoldering and flaming combustions, respectively. As a control, the other group of mice was exposed in an identical chamber to filtered air under the same experimental conditions. Carboxyhemoglobin (COHb) levels were determined in blood of mice collected by puncture of the facial vein immediately before the scheduled end of the second exposure. COHb were analyzed using a CO-Oximeter (Model: 682, Instrumentation Laboratory, Lexington, MA) immediately after the collection.

Ventilatory Function Assessment

Ventilatory function was monitored in unanesthetized/unrestrained mice using whole body plethysmography (Buxco Electronics, Wilmington, NC). Ventilatory function data included: minute ventilation (MV), tidal volume (TV), breathing frequency (F), relaxation time (RT), inspiratory (Ti) and expiratory (Te) time, and peak inspiratory (PIF) and peak expiratory (PEF) flow. Additionally, time and flow rate parameters were used to evaluate an index of ventilator timing (enhanced pause; Penh). To reduce the possibility of homeostatic changes related to time of day, respiratory function data were collected for 27 min at 24 h before exposure (Baseline), immediately after exposure (Day 1 and Day 2), and 24 h after the end of the second day of exposure

(Post), following a 5-min acclimation period for each mouse in its individual plethysmograph. All data were averaged for each 9-min portion of the measurement period.

Lung Toxicity Assessment

At 4 and 24 h after the oropharyngeal aspiration and the end of the second day of the inhalation exposure, mice were euthanized by intraperitoneal injection of Euthasol. Blood was collected by cardiac puncture, and hematology values were measured using a Coulter AcT 10 Hematology Analyzer (Beckman Coulter Inc., Miami, FL). Bronchoalveolar lavage fluid (BALF) was collected from the right lung lobes and used to determine the total cell count and differential analysis of macrophage and neutrophil numbers. We also analyzed the recovered BALF supernatant to determine cellular injury as indicated by protein, albumin, lactate dehydrogenase (LDH), γ-glutamyl transferase (GGT), and N-acetyl-β-D-glucoaminidase (NAG). Pro-inflammatory cytokine responses were assessed by measuring tumor necrosis factor-α (TNF-α), interleukin-6 (IL-6), and macrophage inhibitory protein-2 (MIP-2). Additional details of the biochemical/cytokine analyses are provided in our previous paper (Kim et al. 2018). We calculated the lung toxicity potency by determining the neutrophil counts in BALF (i.e., an equal PM mass basis).

Dosimetry of Inhaled Biomass Smoke PM

We used the publicly available multiple-path particle dosimetry (MPPD, v3.04, Applied Research Associates Inc., Arlington, VA) model to estimate deposition fractions of PM in different compartments (extrathoracic, tracheobronchial, and pulmonary regions) of the mouse respiratory tract during inhalation exposure to the biomass smoke. A detailed description of the MPPD model is given elsewhere (Asgharian et al. 2014). Because the lung toxicity data (e.g., neutrophil numbers in BALF) after inhalation were associated with different PM masses in the respiratory tract, the calculated PM deposition fraction values were used to normalize the lung toxicity response data (# neutrophils/μg PM) so that the toxicity results were comparable at different biomass smoke exposure conditions. In order to further evaluate the toxicity responses of the inhaled biomass smoke PM, we obtained normalized lung toxicity data of the same biomass smoke PM from the aspiration study and compared them with the inhalation toxicity data.

Mutagenicity Assessment

For mutagenicity analysis, we dried the smoke condensate suspension under nitrogen gas, re-suspended the dried smoke condensate in dichloromethane (DCM), and filtered the extractable organic material (EOM). We determined the %EOM by gravimetric measurement and solvent-exchanged the EOM into dimethyl sulfoxide (DMSO). We performed the Salmonella plate-incorporation mutagenicity assay (Maron and Ames 1983) using TA100 and TA98 strains in the presence and absence of metabolic activation using S9 (an aroclor-induced Sprague-Dawley rat liver homogenate). Additional details of the mutagenicity assay are provided in our previous report (Kim et al. 2018). We multiplied the mutagenic potencies of the EOM (rev/μg EOM) by the %EOM to give the mutagenic potencies of the PM (rev/μg PM) for each fuel/combustion condition. We then multiplied these values (rev/μg PM) by the calculated emission factor (EF) for PM (g PM/kg fuel) for each fuel and burning condition to give the mutagenicity EF (rev/kg fuel). We then converted the rev/kg fuel to rev/MJ_{th} using the values for the heat energy of the fuels (MJ_{th}/kg) described above. In order to evaluate the mutagenicity EFs of the biomass smoke in the present study, the rev/MJ_{th} values were compared with the published mutagenicity EFs for red oak

burned in cookstoves as well as for a variety of other emissions available from the literature.

Statistical Analysis

For the analysis of lung toxicity data (pro-inflammatory cytokine, protein, albumin, NAG, LDH and GGT values in BALF, hematology values, and COHb levels), we used one-way analysis of variance (ANOVA) followed by the Dunnett's multiple comparison adjustment to compare the biological responses between PM-exposed groups and a negative control group (saline or filtered air). We modeled the lung toxicity potencies (# neutrophils/µg PM) of the biomass smoke PM with linear regression analysis to characterize their association with different exposure methods (e.g., inhalation and aspiration methods). This analysis was performed using GraphPad Prism software (version 6.07, GraphPad Software, Inc., San Diego, CA). We also modeled neutrophil and Salmonella responses as dependent variables to characterize their association with different fuel types and combustion phases. This analysis was performed using SAS software for Windows (version 9.4, SAS Institute Inc., Cary, NC). For analysis of the neutrophil count data (lung toxicity), we used negative binomial regression in the SAS GENMOD procedure; for analysis of the Salmonella (mutagenicity) responses, we used two-way factorial ANOVA for fixed effects in the SAS MIXED procedure. Negative binomial regression is commonly used for over-dispersed count data, that is, where the variance exceeds the mean, as observed for the neutrophil count data in this study (Lawless 1987). The linear or log scale for statistical tests of the Salmonella responses was determined by evaluating normality of model residuals (Shapiro-Wilk test in SAS UNIVARIATE). We expressed the data as mean ± standard error of the mean (SEM) and assigned the statistical significance level at a probability value of $p < 0.05$.

Lung and Cardiac Toxicity of Biomass Smoke in Rats

Experimental Animals

Adult pathogen-free male Wistar Kyoto rats (Charles River Laboratories Inc.) were housed in polycarbonate cages, maintained on a 12 h light/dark cycle at approximately 22°C and 50% relative humidity in our Association for Assessment and Accreditation of Laboratory Animal Care-approved facility, and held for a minimum of one week before exposure. All rats received standard (5001) Purina pellet rat chow (Brentwood, MO) and water ad libitum unless otherwise stated. The Institutional Animal Care and Use Committee of the U.S. Environmental Protection Agency (U.S. EPA) approved all protocols.

Inhalation Exposure to Peat Smoke

Rats were exposed once for 1 h to the low peat smoke (target concentration = 0.4 mg/m^3) or high peat smoke (target concentration = 4.0 mg/m^3). The low concentration target was chosen based on ambient particulate concentrations typical in highly polluted cities (i.e., Delhi, India) and in order to establish a dose response, we selected the high concentration to be one order of magnitude higher (DPCC 2018). Importantly, this high concentration is on par with respirable particulate matter exposure levels experienced by firefighters while combating wildland fires (Swiston et al. 2008).

Ultrasound Echocardiography

Cardiac function of rats was determined 2 h after high fat (HF) gavage using a high frequency echocardiography ultrasound system (Vevo 2100, FujiFilm Visual Sonics Inc., Toronto, Canada). Rats were first placed in a sealed whole-body chamber and anesthetized with isoflurane.

Once anesthetized, rats were transferred to a heated ECG-monitoring table in dorsal recumbency. An MS-201 transducer was used to noninvasively record 3 video loops of the parasternal long axis views of the left ventricle in M-mode (15 MHz) for functional measurements and pulsed wave Doppler (12.5 MHz) of pulmonary artery and transmitral blood flow. The sonographer was blinded to exposure group identities. We used Vevo® LAB software version 1.7.0 (FujiFilm VisualSonics Inc.) to analyze data collected via pulsed wave Doppler of transmitral flow in order to determine isovolumic contraction time (IVCT), aortic ejection time (AET), and isovolumic relaxation time (IVRT). Additional details of the echocardiography analysis are provided in our previous report (Martin et al. 2018).

Lung and Systemic Toxicity Assessment

The impacts of a single exposure to low and high concentrations of smoldering peat smoke emissions on time-dependent changes in postprandial lipids, hormones, and pulmonary and systemic indicators of inflammation and injury were assessed. The time course of responses post gavage (0, 2 and 6 h) for each exposure group (filtered air, low peat, and high peat) were examined using separate cohorts of rats. At 0 h rats were exposed to smoldering peat smoke or air, fasted overnight, and euthanized at ~8 AM. At 2 h rats were exposed to smoldering peat smoke or filtered air, fasted overnight, and received a HF gavage at 8 AM followed by euthanasia 2 h later. At 6 h rats were exposed to smoldering peat smoke or air, fasted overnight, and received a HF gavage at 8 AM followed by euthanasia 6 h later.

Bronchoalveolar lavage fluid (BALF) was collected from the right lung lobes and used to determine the total cell count and differential analysis of macrophage and neutrophil numbers. The recovered BALF supernatant was also used to determine cellular injury as indicated by protein, microalbumin (MIA), LDH, GGT, NAG. Pro-inflammatory cytokine responses were assessed by measuring TNF-α, IL-6, and MIP-2. Alpha-1 acid glycoprotein (AGP) in serum were also measured for pulmonary and systemic inflammatory responses.

Circulating monocyte phenotype in blood samples was determined using flow cytometry. Blood samples were lysed and labeled with the following monoclonal antibodies: FITC-CD36, PE-CD172a, PE/Cy7-CD11b/c, Alexa Fluor 647-CD43, and APC/Cy7-CD45. After staining, cells were washed and incubated with LIVE/DEAD fixable violet stain to determine viable cells. Cells were washed, fixed with formaldehyde in phosphate-buffered saline (PBS) and kept in the dark at 4 °C (no longer than 1 day) until FACS analysis. All samples were collected on a LSR II flow cytometer (BD Biosciences, San Jose, CA) using FACSDiva software (BD Biosciences). Data analysis was performed by using FlowJo software (TreeStar, Inc., Ashland, OR). A minimum of 50,000 events were collected per analysis. Additional details of the lung toxicity assay are provided in our previous paper (Martin et al. 2018).

Statistical Analysis

Data are reported as boxplots with all data points shown. Box edges mark the interquartile range, the middle line marks the median, the "+" marks the mean, and the whiskers mark the minimum and maximum data values. GraphPad Prism (GraphPad Software version 7.02) was used for all statistical analyses. One-way ANOVA with Tukey's post-test and multiplicity-adjusted p values were conducted for cardiac function data. For all other data a two-way ANOVA non-repeated measure with Tukey's post-test and multiplicity adjusted p values were conducted since t = 0, 2 and 6 h groups were separate cohorts of rats and no serial blood draws were made. A p value < 0.05 was considered statistically significant.

Results and Discussion

Lung Toxicity and Mutagenicity of Biomass Smoke

Properties of Smoldering and Flaming Combustion Emissions

Specific properties, including MCE, PM size distribution, PM concentration, and pollutant EFs, of the smoke from five biomass fuels (red oak, peat, pine needles, pine, and eucalyptus) and two combustion phases (smoldering and flaming) are listed in Table 1. The MCE values were 63 - 83% during the smoldering and 97 - 99% during the flaming phase. For all fuel types, the median diameters for the PM based on surface area-weighted particle size distributions from the smoldering phase were >1 μm (mean = 2.04 μm), whereas those from the flaming phase were <1 μm (mean = 0.59 μm).

The mean ± SEM of the EFs for CO, CO_2, and PM of the smoldering phase smoke was 233±26, 1,026±74, and 121±16 g/kg fuel, respectively, whereas the average EFs for CO and PM of the flaming phase smoke were decreased to 22±3 and 1±0 g/kg fuel, respectively. In contrast, the average EF for CO_2 increased with flaming combustion to 1,795±5 g/kg fuel. These data confirm that the flaming combustion conditions were more efficient, converting much of the carbon to CO_2, whereas more carbonaceous PM and CO were emitted during smoldering.

Table 1. Characteristics and EFs of the biomass smoke emitted from the tube furnace system.

Variable	Red oak		Peat		Pine needles		Pine		Eucalyptus	
	Smoldering	Flaming	Smoldering	Flaming	Smoldering	Flaming	Smoldering	Flaming	Smoldering	Flaming
Characteristic										
MCE (%)	73±1	99±0	71±1	97±0	83±0	98±0	76±1	98±0	63±1	98±0
PM size (μm)[a]	1.38[1.22]	0.65[2.09]	2.73[1.41]	0.89[2.96]	2.70[1.40]	0.54[1.27]	2.37[2.76]	0.40[1.46]	1.02[2.90]	0.48[1.41]
CO (ppm)	793±30	80±6	1,385±135	159±10	602±34	121±8	766±25	105±14	1,201±53	109±10
CO_2 (ppm)	2,167±111	5,597±173	3,425±373	5,042±161	3,067±192	6,576±161	2,458±120	6,844±222	2,058±67	6,407±160
PM (mg/m^3)	973	8	488	15	624	18	1,050	14	1,418	10
Emission factor										
CO	231	16	288	33	154	20	198	21	292	20
CO_2	990	1,804	1,120	1,777	1,233	1,797	999	1,797	787	1,798
PM	131	1	71	1	98	1	143	1	160	1

[a]Surface median aerodynamic diameters calculated from surface area-weighted particles size distributions; values in brackets represent the geometric standard deviation (GSD) of the particle size distributions

We plotted the pollutant EFs for CO, CO_2, and PM as a function of the MCE and compared their relationships with published field and laboratory measurement data (Figure 4). Except for the EFs developed for smoldering peat, EFs were linearly dependent on the MCE of each fuel, and the linear trends were fitted to the published data obtained from above-ground fuel combustions (r^2 = 0.97, r^2 = 0.82, and r^2 = 0.86 of EFs for CO, CO_2 and PM, respectively) (McMeeking et al. 2009). Although the EFs of the peat smoke fell outside the linear trend lines, and this deviation increased in the plot of the EF for PM versus the MCE, they were in good agreement with the published EFs of smoldering phase smoke from ground fuel combustions (e.g., duff and organic soils) (Urbanski 2014) and peatland wildfires (Geron and Hays 2013) (r^2 = 0.83, r^2 = 0.93, and r^2 = 0.61 of EFs for CO, CO_2 and PM, respectively) (Figure 2). We also found that the correlations were distinguished by specific fuel types (e.g., above- and in-ground fuels); note that the y-intercepts of the regression lines for the pollutant EFs as a function of MCE were quite different between the two fuel types

(Figure 4). This suggests that there are distinct differences in the emission characteristics from biomass fuels from in- versus above-ground. Comparing our data to previously published values also suggests that pollutant EFs from controlled or uncontrolled combustion of biomass are highly dependent on the distribution of the biomass fuels vertically (above-ground or in-ground) rather than horizontally (i.e., the Genus or family of wood or biomass).

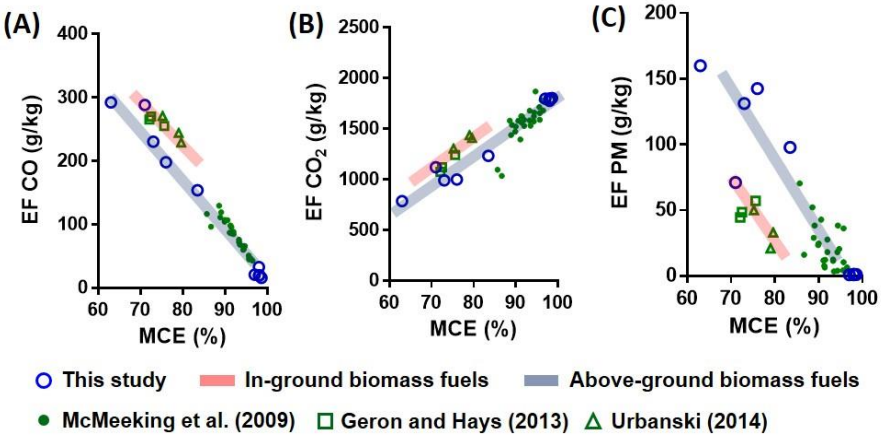

Figure 4. Comparison of EFs estimated from the tube furnace system in this study with published EFs from various fuel combustions. (A) – (C) pollutant EFs for CO, CO_2, and PM versus modified combustion efficiency (MCE).

The cryotrap sampling system collects and composites chemical compounds across a wide volatility range. Thus, the cryotrap samples were expected to be quite different from those collected using traditional filter-based PM and gas-phase sampling methods, which typically attempt to separate compounds by chemical and physical state. The use of the cryotrap allowed us to collect volatile and semi-volatile organic compound emissions in a single sample, eliminating the well-known artifacts and interferences associated with classical sample collection (McDow and Huntzicker 1990). It also allowed us to more accurately predict specific chemical components associated with exposures to biomass smoke.

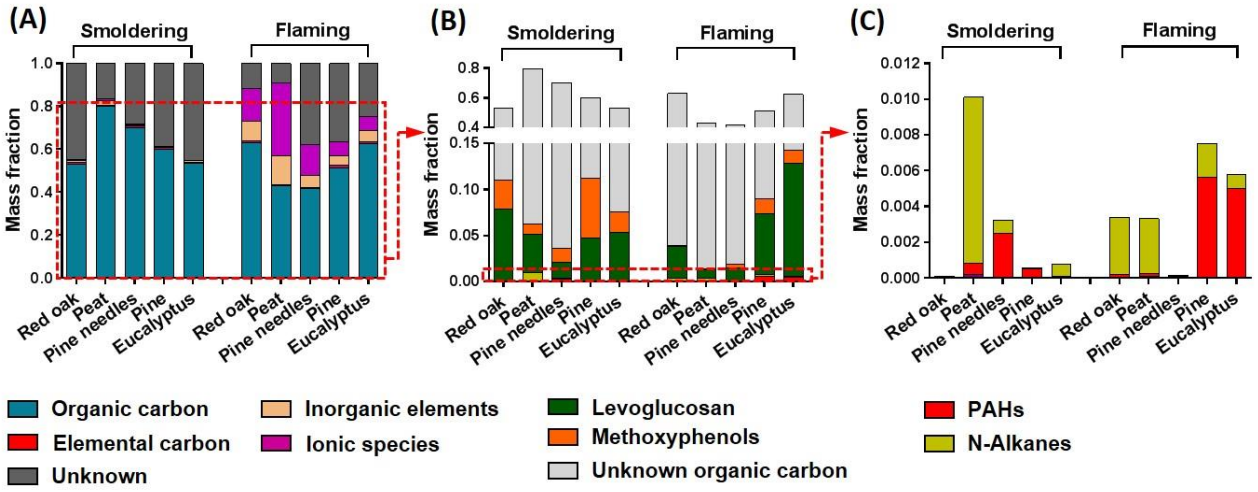

Figure 5. Chemical components in the biomass smoke condensate collected from different fuel types and combustion phases. (A) mass fraction of major chemical compounds, (B) organic carbon species (the red dashed line, superimposed on (A)), and (C) semi-volatile compounds (the red dashed line, superimposed on (B)) in the biomass smoke condensate from smoldering and flaming combustion.

The major chemical compounds measured in the biomass smoke condensate samples are shown in Figure 5 and Table 2. Depending on the sample, the smoldering combustion emitted 4 - 49 times more PM (or dried smoke condensate) mass than flaming combustion, but endotoxin (average of 329 and 241 EU/g for smoldering and flaming, respectively) and pH levels (average of pH 3.57 and 3.67 for smoldering and flaming, respectively) of the PM were similar on a mass basis between the two combustion conditions (Table 2). The wood smoke condensate samples (i.e., red oak, pine, and eucalyptus) averaged 56 and 60% (of PM mass) total carbon for smoldering and flaming, respectively, whereas the non-wood smoke condensate samples (i.e., peat and pine needles) had a slightly higher percentage of total carbon for smoldering (average of 76 % of PM mass) but lower for flaming (average of 43% of PM mass) combustion. This value is similar to observations made by Kim et al. (2014), who found that PM samples from the peat-bog wildfire were comprised of 53.4% organic matter. Similarly, Reid et al. (2005) reviewed the properties of biomass burning particles and found that the percentage of fresh smoke particles to which OC contributed varied from 13.6 – 67% depending on the biomass type and combustion phase.

Table 2. Chemical compositions of the biomass smoke condensate collected from the cryotrap system.

Component (unit)	Red oak		Peat		Pine needles		Pine		Eucalyptus	
	Smoldering	Flaming	Smoldering	Flaming	Smoldering	Flaming	Smoldering	Flaming	Smoldering	Flaming
PM mass (mg)	488	10	117	28	449	27	789	25	955	21
EOM[a] (% of PM mass)	50	47	73	38	62	35	60	43	52	40
pH	3.37	3.78	4.26	3.17	3.85	3.51	3.08	3.92	3.30	3.98
Endotoxin (EU/g)	449	249	270	161	343	232	321	256	262	306
Ion (µg/g)	1,285	155,982	7,148	339,077	3,379	143,418	949	66,625	330	65,259
Ion (% of PM mass)	0	16	1	34	0	14	0	7	0	7
Organic carbon (µg/g)	529,508	629,242	797,863	430,830	699,443	416,413	601,394	513,893	532,723	624,508
Elemental carbon (µg/g)	7,787	8,160	8,120	3,968	7,795	2,774	5,070	12,509	5,026	10,081
Carbon (% of PM mass)	54	64	81	43	71	42	61	53	54	63
Element (µg/g)	11,081	91,367	20,559	131,583	5,505	56,962	5,920	42,788	8,045	51,879
Element (% of PM mass)	1	9	2	13	1	6	1	4	1	5

[a]Extractable organic matter (EOM) represents nonvolatile organic material present in the biomass smoke PM that was extracted by dichloromethane.

Ionic species (mostly Cl^-, SO_4^{2-}, and PO_4^{3-}) accounted for <1% and 15.6% of PM in the smoke condensate samples from smoldering and flaming combustion, respectively (Figure 5). Similarly, inorganic species (mostly Ca, Na, S, and metals) of the smoke condensate collected from smoldering contributed to an average of 1% of PM mass and inorganic species from flaming samples contributed to an average of 6% of PM mass (Figure 5). The peat flaming smoke condensate contained the highest level of heavy metals (e.g., Cr, Cu, Fe, Ni, Pb, Sb, and Zn), accounting for up to 1.2% of PM mass. For both the flaming and smoldering conditions, the wood smoke condensate was enriched in levoglucosan (up to 12.6% of PM mass) compared with the non-wood smoke condensate (up to 4.1% of PM mass), whereas total methoxyphenols made up a higher percentage of the PM mass in smoldering smoke condensate (up to 6.5% of PM mass) than in flaming smoke condensate (up to 1.6% of PM mass) for all fuel types (Figure 5). Levels of n-alkanes and PAHs in the smoke condensate samples also varied on the basis of combustion conditions and fuel type (Figure 5). Previous studies show that PAH concentrations in wood smoke PM increase with combustion temperature (Bolling et al. 2012; McDonald et al. 2000; McMahon

and Tsoukalas 1978; Reid et al. 2005). Here the PAH concentrations in the wood smoke condensate (red oak, pine, eucalyptus) were higher for flaming conditions; however, for the non-wood fuels (peat and pine needles) PAHs were higher for smoldering conditions. Furthermore, higher combustion temperatures during flaming also increased the amount of ionic and inorganic species in the smoke condensate from flaming compared to smoldering conditions in agreement with a report showing that trace element concentrations for hot burning woods were two orders of magnitude higher than those for cool burning woods (Rau 1989). Similarly, Frey et al. (2009) reported that wood burning at high temperatures was associated with high emissions of ions and trace elements (20 and 1% of EF for PM, respectively) compared to low temperature combustion (2 and 0.3% of EF for PM, respectively). Collectively, our findings show that the chemical composition of biomass smoke varies substantially depending on flaming or smoldering conditions and on fuel types, especially between wood or non-wood biomass fuels.

While it could be argued that the biomass smoke generated from our system is less complex than natural wildland fire smoke, the precise control offers better reproducibility of biomass smoke production from other laboratory- or field-based open burning combustions that generate less consistent biomass smoke, limit understanding of specific combustion conditions, and hinder comparison across studies. In this regard, the strength of our combustion system is that it can be used to generate well-defined and reproducible biomass smoke that is suitable for use as a reference material in future laboratory studies

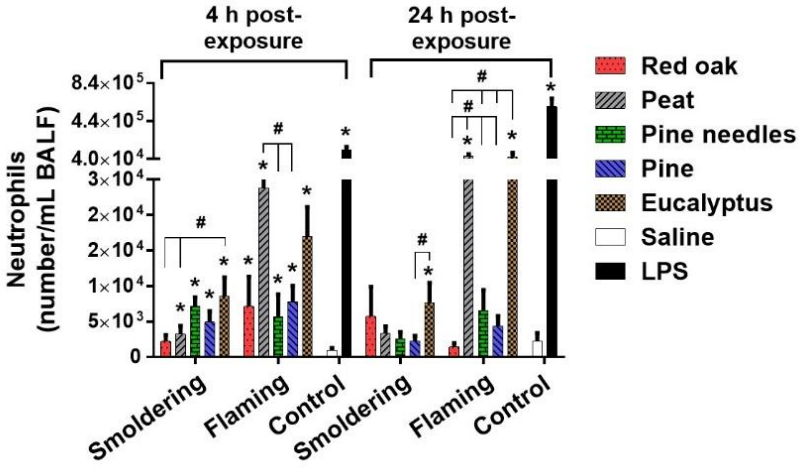

Figure 6. Comparative lung toxicity potencies of the biomass smoke PM emitted from different fuel types and combustion phases.

Lung Toxicity of Aspirated Biomass Smoke PM

Neutrophil counts (per mass of PM) were highest in mice exposed to the flaming peat and eucalyptus PM at 4 h (Figure 6). The average proportion of neutrophils relative to the total number of BALF cells was 22% following both exposures, compared with only 2% in controls at 4 h. At 24 h, BALF neutrophil counts in the mice exposed to the flaming peat and eucalyptus PM were higher than (or similar to) counts in exposed mice evaluated at 4 h, and neutrophils accounted for 44 and 21% of total lavageable cells on average, respectively, compared with 2% in controls (Figure 6). The flaming peat and eucalyptus PM were associated with significantly higher neutrophil response than other fuel PM samples at 24 h post-exposure. The total numbers of macrophages were similar for each PM sample in mice evaluated 4 and 24 h post-exposure (data

not shown). Lung injury and inflammation can be triggered by a number of different signals from both inorganic and organic moieties that cause oxidative stress in one form or another (Bolling et al. 2009; Bolling et al. 2012). The flaming peat sample had the highest levels of heavy metals (Cr, Cu, Fe, Mn, Ni, Pb, Sb, and Zn) and sulfate, many of which have been implicated in lung injury and inflammation through increased redox cycling (Fang et al. 2017; Gavett et al. 1997; Happo et al. 2013; Reiss et al. 2007; Veranth et al. 2006). On the other hand, the flaming eucalyptus had the highest levels of certain PAHs, such as phenanthrene, anthracene and fluoranthrene; the capacity for PAHs to induce oxidative stress through quinone formation is well documented (Bolling et al. 2009). The acute toxicity of eucalyptus smoke has also been linked specifically to phenolic compounds such as phenol and o-cresol (Pimenta et al. 2000).

Further analysis of pro-inflammatory cytokines in BALF revealed that the concentrations of IL-6, TNF-α, and MIP-2 were significantly elevated in mice exposed only to the flaming peat PM at 4 h, compared with control mice evaluated at the same time point (data not shown). Although the number of neutrophils was higher in mice evaluated at 24 h than in mice evaluated at 4 h post-exposure to the flaming peat, the concentrations of TNF-α and MIP-2 were lower at 24 h, and not significantly different from saline controls. The concentration of IL-6 was also lower in mice evaluated at 24 h than in mice evaluated at 4 h post-exposure, but it remained significantly higher than in saline controls. For mice exposed to the flaming peat PM, the concentrations of protein, albumin, NAG, LDH, but not GGT, in BALF were significantly higher than saline controls evaluated at 24 h, but were not significantly different from saline controls evaluated at 4 h post-exposure (data not shown).

Hematology analysis showed that, compared with controls, mice exposed to the smoldering eucalyptus PM had significantly lower white blood cell counts, and mice exposed to the smoldering pine PM or eucalyptus PM had significantly lower lymphocyte counts at 4 h post-exposure. Mice exposed to the flaming peat, pine needles, pine, and eucalyptus PM had significantly lower white blood cell and lymphocyte counts at 4 h post-exposure. At 24 h post-exposure, while blood cell and lymphocyte counts were not significantly different from controls (data not shown). Other hematology values (e.g., red blood cell counts, hemoglobin, and hematocrit) were not significantly different between exposed mice and controls at 4 h or 24 h post-exposure.

Mutagenicity of Biomass Smoke PM

The highest mutagenic potencies of the PM (rev/μg PM) were those from flaming peat and pine, and their potencies were also significantly higher than those of the majority of other fuel PM in both strains +/-S9 (Figure 7). Similar to the lung toxicity potencies (neutrophils/mass of PM), the mutagenic potencies of the PM (i.e., on a mass basis) were far higher under flaming phases than from smoldering phases. Of the flaming samples, the increase in the mutagenic potency of peat without S9 was higher than other fuel types, suggesting that unlike wood smoke, the organic components from peat smoke were primarily direct-acting mutagens in the Salmonella assay. The higher mutagenic potencies of the PM samples in TA100 versus TA98 were consistent with findings from other studies of wood smoke (Asita et al. 1991; Mutlu et al. 2016), suggesting that the base-substitution mutagenic activity was generally more prominent than frameshift activity for these PM samples.

The mutagenic potencies of the PM for each biomass fuel in each strain was similar with and without metabolic activation (+S9 and -S9, respectively), consistent with a mix of direct- and indirect-acting mutagenic activity. However, the PM from each biomass fuel was typically more

mutagenic in TA100 than in TA98, consistent with mutagenicity due to base-substitution (versus frameshift) mutations. All the mutagenic potencies of the PM in this study were significantly associated with different fuel types and combustion phases ($p < 0.01$).

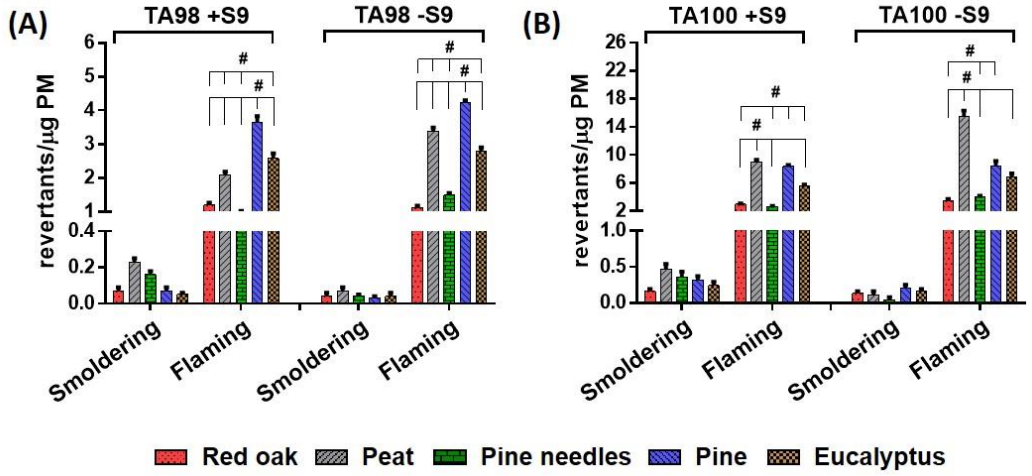

Figure 7. Comparative mutagenic potencies of the biomass smoke PM emitted from different fuel types and combustion phases. (A) - (B) mutagenic potencies in strains TA98 +/-S9 and TA100 +/-S9 calculated based on the equal PM mass.

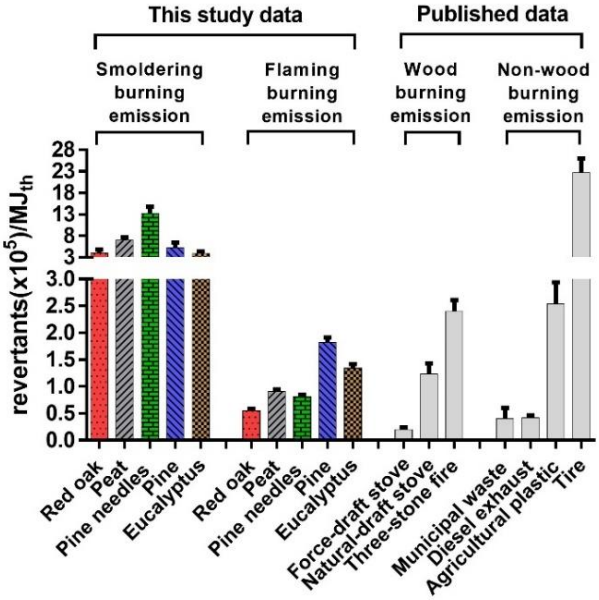

Figure 8. Comparison of mutagenicity emission factors (EFs) of various combustion emissions in strain TA98 +S9.

Mutagenicity Data Comparison of Biomass Smoke with Other Combustion Smoke

We determined mutagenicity EFs based on fuel energy used (rev/MJ_{th}) and compared these with the published mutagenicity EFs for various combustion emissions obtained from TA98 +S9 (Figure 8). The mutagenicity of the flaming emissions (1.1×10^5 rev/MJ_{th}; average of the five fuel burning emissions) was relatively similar to that of wood-burning cookstove emissions (1.3×10^5 rev/MJ_{th}; average of force-draft stove, natural-draft stove, and three-stone fire emissions; (Mutlu et al. 2016)). Although the smoldering emissions (6.6×10^5 rev/MJ_{th}; average of the five fuel

burning emissions) were less mutagenic than the emission from the open burning of tire (22.7×10^5 rev/MJ_{th}; (DeMarini et al. 1994)), they were more mutagenic than those of diesel exhaust (0.4×10^5 rev/MJ_{th}; (Mutlu et al. 2015)), municipal waste combustion (0.4×10^5 rev/MJ_{th}; (Watts et al. 1992)), and the open burning of agricultural plastic (2.5×10^5 rev/MJ_{th}; (Linak et al. 1989)). Thus in this context, the smoldering emissions from wildland fires are highly mutagenic and support the notion that smoldering wood smoke is genotoxic and ultimately carcinogenic in humans (IARC 2010; Kato et al. 2004; Long et al. 2014).

Lung Toxicity of Inhaled Biomass Smoke

Properties of Smoldering and Flaming Smoke in the Inhalation Chamber

Average PM concentrations for the biomass smoke exposures were 40.5 mg/m^3 during the smoldering (85% of MCE) and 3.7 mg/m^3 during the flaming phase (98% of MCE), and the PM levels stayed within 1 – 5% of the smoldering and 5 – 15% of the flaming phase target set value over the entire exposure period (Figure 9 and Table 3). Under the two distinct levels of PM in the inhalation chamber, CO levels ranged from approximately 60 to 110 ppm for all the biomass smoke emissions. NOx levels in the flaming smoke were approximately 30 – 70 times higher than those of the smoldering smoke while selected VOC levels were up to approximately 3 times higher in the smoldering smoke. Mass median aerodynamic diameters of PM in the biomass smoke ranged from 0.1 – 0.3 µm with low GSD values (approximately 1.43) for all tested fuel combustion emissions. This is consistent with previous reports on the particle sizes of similar wood smoke (Kleeman et al. 1999). Reid and Hobbs (1998) reported that fresh smoke particles emitted from forest fires with different vegetation and changing combustion phases had a size range from 0.2 to 0.3 µm, and further suggested that particle size in the biomass smoke appear to be mainly governed by condensation and coagulation processes rather than combustion intensity.

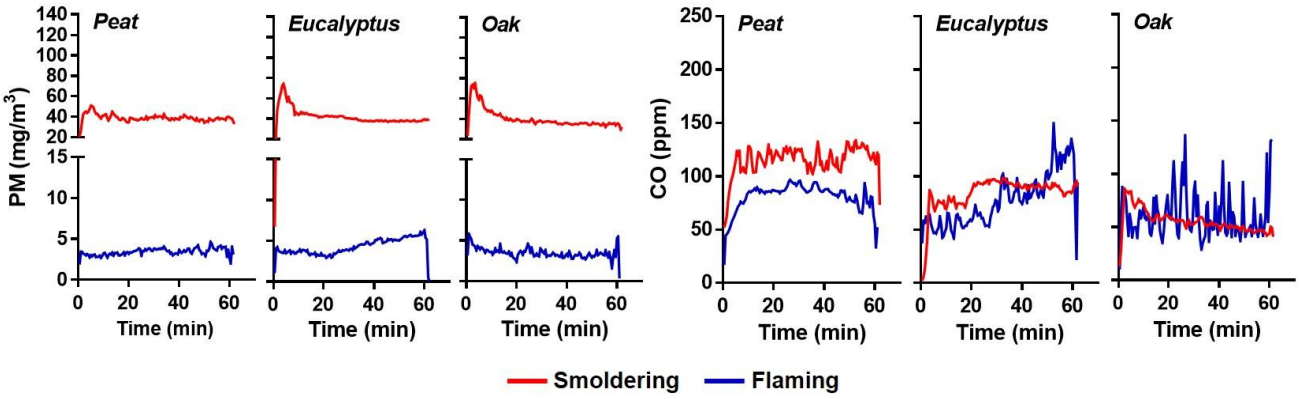

Figure 9. Average concentrations of PM and CO of the biomass smoke in the inhalation chamber during exposures.

Although the different combustion conditions (e.g., fuel types and burning temperatures) presented here minimally affected particle size, they had profound effects on chemical properties of the biomass smoke. Major chemical characteristics of particulate- and gas-phase compounds in the biomass smoke are shown in Figure 10A. Total carbon accounted for 40 – 70% of PM mass from all three fuels from either the smoldering or the flaming phase. Ionic species and inorganic elements each constituted approximately 1% of the PM mass from smoldering combustion, but constituted approximately 5% of the PM mass from the flaming phase presumably because the increased combustion temperature promotes the vaporization of ionic and inorganic species (Frey

et al. 2009; Rau 1989). Likewise, flaming combustions also led to higher NOx emissions (Jaffe and Wigder 2012) although this is also influenced by increased nitrogen content in the fuels, particularly with peat, resulting in increased NOx emissions compared to other biomass combustions in this study (Lacaux et al. 1996). The highest levels of VOCs were measured in the oak smoke (smoldering or flaming), whereas the eucalyptus flaming smoke contained the lowest VOC levels (Figure 10B). Major VOC components were acetaldehyde (up to ~25% of VOCs in all smoldering exposures), acrolein (~15% of VOCs in flaming peat smoke), formaldehyde (~43% of VOCs in flaming eucalyptus smoke), and benzene (~30% of VOCs in flaming oak smoke). Unlike ions, elements, and NOx production, VOC emissions showed the opposite trend, with higher emissions from the smoldering than the flaming combustion. Greenberg et al. (2006) reported that the reaction of oxygen with organic content in the biomass fuel at low combustion temperatures (approximately 300°C) produced high VOC emissions, while the oxidation at high temperatures (>500°C) generated low VOC with high CO_2 emissions.

Table 3. Characteristics of the biomass smoke in the inhalation chamber.

Characteristic (unit)	Peat		Eucalyptus		Oak	
	Smoldering	Flaming	Smoldering	Flaming	Smoldering	Flaming
MCE (%)	86±1	97±0	84±1	98±0	84±0	98±0
PM (mg/m^3)	38.7±0.4	3.4±0.1	42.2±0.6	4.2±0.1	40.5±0.8	3.5±0.1
CO (ppm)	115±1	81±1	84±2	76±2	56±1	59±2
CO_2 (ppm)	721±5	2,794±40	427±8	4,790±78	297±5	2,942±65
NO (ppb)	227±54	5,109±892	30±1	1,449±61	39±0	1,812±233
NO_2 (ppb)	0±0	1,292±187	0±0	666±19	0±0	502±154
NOx (ppb)	227±54	6,380±1,079	30±1	2,106±77	39±0	2,303±384
VOCs (ppb)	2,677	1,694	1,911	760	4,072	1,682
MMD (nm)[a]	151[1.46]	133[1.29]	283[1.46]	165[1.40]	180[1.52]	158[1.32]

[a]Mass median diameter (MMD) of PM; values in brackets represent the geometric standard deviation (GSD)

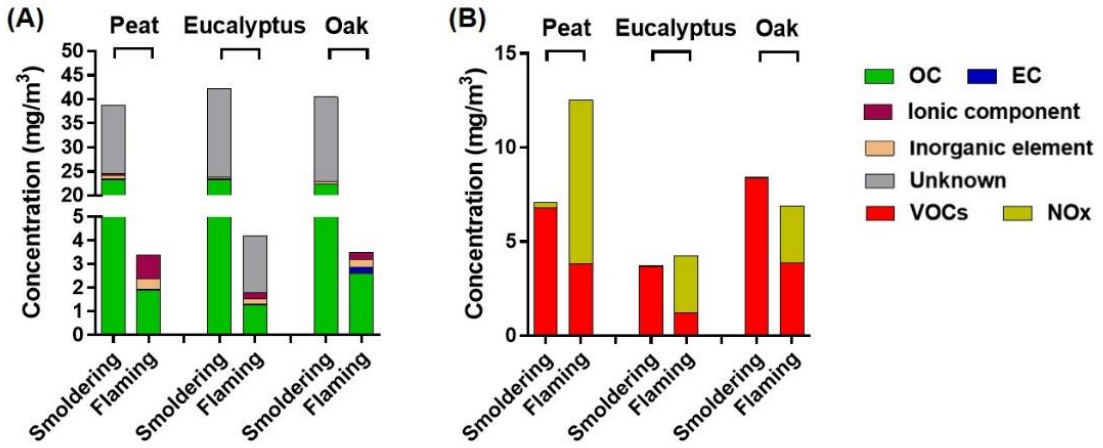

Figure 10. Major chemical components of the biomass smoke in the inhalation chamber during exposures. (A) particulate-phase chemical components. (B) gas-phase chemical components.

Lung Toxicity of Inhaled Biomass Smoke

Since this study mainly focused on toxicity effects of PM in the biomass smoke, it was also critical to avoid potential interfering health effects of inhaled CO during exposures. COHb levels in blood of mice exposed to the biomass smoke for 1 h ranged from approximately 7 to 13% and

corresponded reasonably well to the exposure concentration pattern (approximately 60 to 110 ppm CO) (Figure 11A). Numerous studies have provided evidence that CO exposure differentially and selectively mediates anti-inflammatory and pro-inflammatory effects (Dolinay et al. 2004; Goebel et al. 2008; Otterbein et al. 2000; Wilson et al. 2010). Specifically, Otterbein et al. (2000) demonstrated that CO exposures at intermediate concentration (250 ppm CO for 2 h) inhibited expression of pro-inflammatory cytokines (TNF-α, IL-1β and MIP-1β) and also induced expression of anti-inflammatory cytokine (IL-10) in vitro and in an in vivo mouse model (after stimulation by lipopolysaccharide (LPS)). However, CO concentrations in the biomass smoke produced during this study were maintained at a lower level (60 – 110 ppm, average 79 ppm CO) and allowed for better evaluation of lung toxicity associated with PM and other gas phase constituents. In fact, blood COHb levels (7 – 13%) in the smoke exposed mice were lower than the biological threshold limit value (15 – 20% in human and 15 – 30% in rodents) (Foresti et al. 2008; Wilson et al. 2010), supporting that CO-mediated toxicity was not likely to occur over the course of exposure in this study.

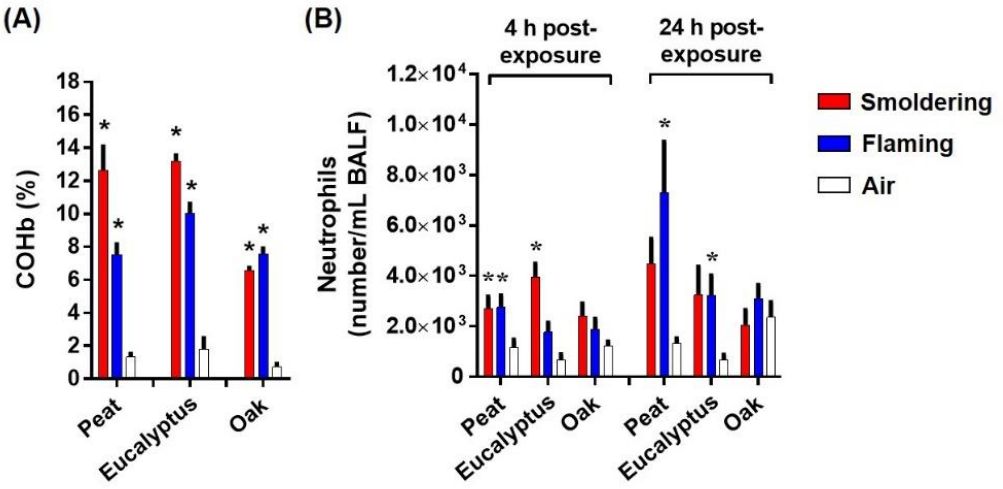

Figure 11. Biological responses in mice exposed to the biomass smoke. (A) COHb levels in blood of mice exposed to the biomass smoke. (B) neutrophil numbers in BALF of mouse lungs exposed to the biomass smoke.

At 4 and 24 h after the end of the second day of exposure, BALF of the mice was analyzed for various biomarkers of lung cell injury and inflammation. A small but significant increase in neutrophil influx into the lung was observed in mice exposed to the smoldering peat and eucalyptus and flaming peat smoke at 4 h post-exposure, with the neutrophil response further increasing (up to ~6% of total BALF cells) at 24 h after the flaming peat and eucalyptus smoke exposures (Figure 11B). The fact that eucalyptus flaming smoke had the highest health effects with relatively lower NOx however suggests that NOx did not contribute as much as other components. It should be noted that despite the ten-fold lower PM concentration of the flaming smoke, the mice exhibited significantly increased neutrophil numbers in the lungs at 24 h post-exposure further confirming that the lung toxicity of biomass smoke emissions on a PM mass basis are greater from the flaming than the smoldering phase. Neutrophil numbers were not significantly increased at 4 and 24 h after exposure to the oak smoke from either smoldering or flaming combustion. Total numbers of macrophages in BALF were largely unchanged for any biomass smoke at 4 and 24 h post-exposure (data not shown). While the number of neutrophils rose under inhalation exposures to certain types of the biomass smoke, levels of pro-inflammatory cytokines in BALF were not significantly

elevated at any of the biomass smoke exposure conditions (data not shown). We also showed significant increases in pro-inflammatory cytokine responses in the lungs exposed to the flaming smoke PM by the aspiration method, and surmise that bolus instillation (aspiration) may have resulted in increased initial signaling even though the resulting inflammatory responses were quantitatively quite similar (Driscoll et al. 2000). Small (but significant) increases in lung injury biomarkers (protein, albumin, LDH, and GGT) were observed for the peat (smoldering and flaming) and eucalyptus (flaming) smoke but not the oak smoke exposure (data not shown). None of the smoke exposures significantly altered any of the hematological parameters studied (data not shown).

Ventilation Parameters following Biomass Smoke Inhalation

Changes in respiratory (ventilation) parameters (Te, Ti, PIF, PEF, RT, MV, TV, and F) in mice were monitored prior to the biomass smoke exposure (baseline), immediately after each day of exposure (Day 1 and Day 2), and at 24 h after the second day of exposure (Post). All respiratory parameters are expressed as a percentage (%) after normalization to the average pre-exposure values (baseline values). Based on the recorded measurements for PEF, PIF, Te, and RT, changes in ventilatory timing (as measured by Penh) associated with the biomass smoke exposure were calculated (Figure 12). Overall, a significant increase in ventilatory timing, potentially indicating airflow obstruction, was observed in mice exposed to the flaming peat smoke (Day 2) and both flaming and smoldering eucalyptus smoke (Day 1, Day 2, and Post), while the flaming and smoldering oak smoke at approximately the same CO and PM concentrations did not significantly alter ventilatory timing after each day of exposure (Day 1 and Day 2). Since there were no meaningful differences in gas phase components (i.e., VOCs, CO and CO_2) among the peat, eucalyptus, and oak biomass smoke under the same combustion phase, the significant ventilatory alterations following exposure to the peat and eucalyptus smoke appeared to be mainly associated with PM phase components. However, the high NOx concentration (6.4 ppm) may have contributed to changes in lung function of mice exposed to the flaming peat smoke (Kleinman and Mautz 1991). The lack of ventilatory alterations of the oak smoke exposure is consistent with our previous report (Gibbs-Flournoy et al. 2018) suggesting that smoke from this fuel is less toxic than from the other fuels tested. Since this study only assessed lung toxicity after acute inhalation exposures, further research is needed to determine if the differential toxicity is still valid for long-term exposures.

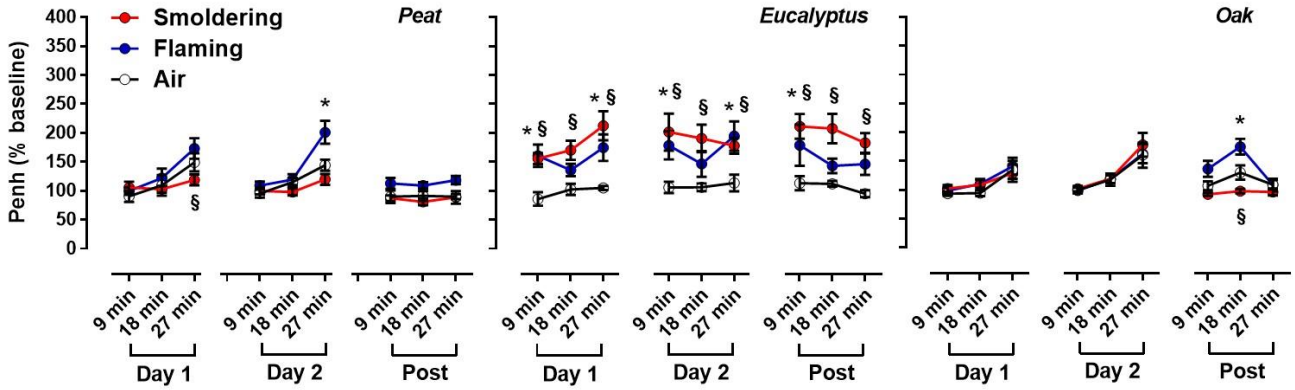

Figure 12. Ventilatory function of mice exposed to the biomass smoke.

Evaluation of Dose Dependent Responses to Biomass Smoke

The percent of PM deposited in the respiratory tract following inhalation exposure was estimated with the MPPD model using empirical input parameters and calculated to be 0.32 – 0.39 for the various exposure conditions (Figure 13A). Based on this modeled value, lung toxicity potency (i.e., neutrophil numbers normalized by the deposited PM mass in the respiratory tract) of the biomass smoke PM after the inhalation exposure was calculated and compared with the lung toxicity potency of PM in the aspiration exposure study. The deposited dose of inhaled PM in the inhalation exposure study was calculated to be 75 μg for the smoldering smoke PM (deposited dose = deposited fraction of the inhaled PM in the respiratory tract (0.34) × PM concentration (40.3 mg/m^3) × duration of exposure (2 h) × minute ventilation of the mice (46 L/min)) and relatively comparable to the deposited dose of aspirated PM (81 μg; assuming a respiratory tract deposition fraction of 81% by an aspiration method (Foster et al. 2001)) described above. Like the results from the aspiration exposure study, the flaming biomass smoke (per unit mass of PM) from peat and eucalyptus fuels was associated with significantly higher neutrophil response than the smoldering smoke. This finding was further supported by linear regression analysis of the lung toxicity potencies between two exposure methods (Figure 13B). A good correlation of the lung toxicity potencies between the inhalation and aspiration methods was observed in mice exposed to the peat ($p < 0.001$) and eucalyptus ($p = 0.0058$) smoke. However, since the lung toxicity associated with the oak smoke exposures was not significant, the inhalation and aspiration exposure outcomes did not correlate with each other ($p = 0.3250$).

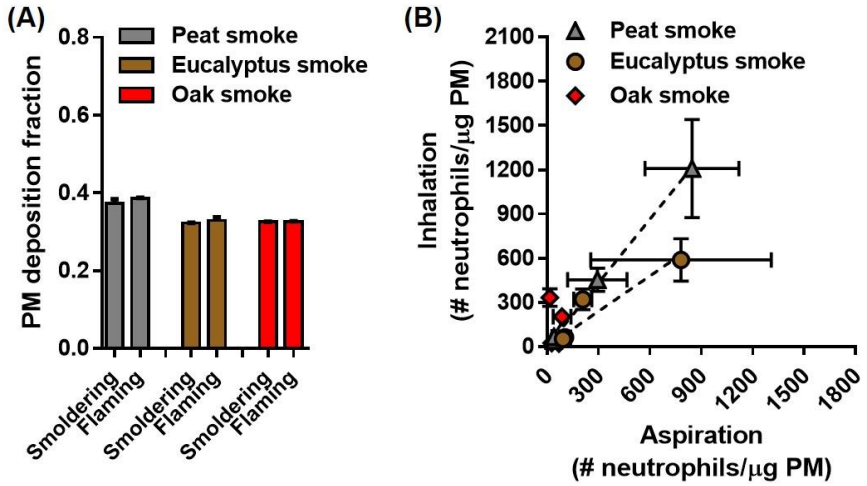

Figure 13. Dosimetric analysis of lung toxicity of inhaled biomass smoke PM in mice.

Lung and Cardiac Toxicity of Inhaled Biomass Smoke

Characteristics of Peat Smoke

Table 4 shows the composition of the peat smoke. Actual PM concentrations for the high and low peat smoke (i.e., 3.3 mg/m^3 and 0.36 mg/m^3) were slightly lower than target concentrations of 4.0 mg/m^3 and 0.4 mg/m^3. High peat smoke had, on average, greater particle number and greater particle size. Low peat smoke, in contrast, had greater had a greater percentage of organic carbon. High peat smoke had approximately 5-fold the amount of CO and 2-fold the level of NOx, although the levels of each gas were very low in each exposure group. High peat smoke also had slightly higher CO_2 levels.

Table 4. Characteristics of the peat smoke in the inhalation chamber.

	PM (mg/m^3)	CO (ppm)	CO_2 (ppm)	NOx (ppb)	Size (µm)	Number (#/cc)	OC (% PM mass)	EC (% PM mass)
Low Peat	0.36±0.00	2.45±0.06	659±8	3.9±0.3	0.71±0.07	3,714±739	76.9±15.3	0.0±0.0
High Peat	3.30±0.04	11.55±0.22	907±4	8.3±0.4	1.3±0.2	4,562±1,108	67.6±5.4	0.4±0.0

Cardiac Effects of Peat Smoke after High Fat (HF) Gavage

Figure 14 shows changes in cardiac function 2 h after HF gavage. Low peat smoke increased isovolumic relaxation time (IVRT) compared to both filtered air ($p < 0.05$) and high peat smoke ($p < 0.05$), but there were no significant effects of exposure on isovolumic contraction time (IVCT) and aortic ejection time (AET). This effect usually indicates poor myocardial relaxation and impaired diastolic function in humans (Gibson and Francis 2003). Furthermore, these data are consistent with reported effects of air pollutant exposure in humans and experimental models. For example, passive smoking was linked to impaired left ventricular diastolic function in healthy volunteers (Dogan et al. 2011) and tobacco smoke exposure over the course of 5 weeks increased IVRT in rats (Gu et al. 2008). There were few other cardiac effects of exposure and although there was also no measurable change in superior mesenteric artery flow after exposure, use of techniques that focus on endothelial or microvascular function in future studies may more readily uncover vascular effects of exposure.

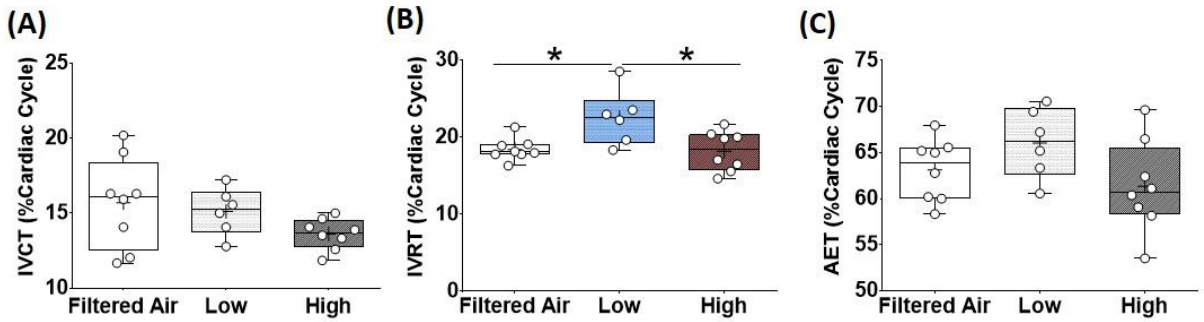

Figure 14. Cardiovascular function in peat smoke-exposed rats measured at 2 h post gavage. (A) IVCT (isovolumic contraction time), (B) IVRT (isovolumic relaxation time), (C) AET (aortic ejection time).

Lung and Systemic Toxicity of Peat Smoke after High Fat (HF) Gavage

Peat smoke impacts on pulmonary and systemic markers of inflammation and injury measured in ungavaged rats at 0 h or after HF gavage are shown in Figure 15. There were no effects of peat smoke exposure on lung MIA levels within each of the measured time points. MIA levels in the high peat smoke group at 2 h post-gavage, however, were higher than levels in the corresponding group at 0 h (Figure 15A; $p < 0.05$). There were no effects of peat smoke exposure on lung GGT levels at 0 h. In contrast, both low and high peat smoke increased lung GGT levels relative to filtered air at 2 h (Figure 15B; $p < 0.05$). Lung GGT levels in the air group at 2 h post-gavage were less than the levels in the corresponding group at 0 h, whereas GGT levels in the low peat smoke group at 2 h were greater than levels in the corresponding group at 0 h ($p < 0.05$). Given that HF meals on their own alter pulmonary function (Rosenkranz et al. 2010), these findings suggest that exposure to air pollution may prime the respiratory tract to heightened responses to pro-inflammatory triggers including HF meals. Although GGT is typically associated with the synthesis of glutathione in liver and kidneys (Goldberg 1980), it plays an important role in regulating oxidative stress in the lungs (Jean et al. 2003), and may indicate some level of lung

injury and inflammation, since an increase in GGT has been shown to be associated with increases in proinflammatory cytokines. For example, intra-pulmonary administration of organic extracts of PM collected from a peat wildfire in North Carolina also caused an increase in GGT in mice (Kim et al. 2014). There were little to no effects of exposure and/or gavage on other indicators of pulmonary injury and inflammation (data not shown). There were no effects of peat smoke exposure on serum AGP levels at 0 h or 6 h post-gavage (Figure 15C). In contrast, high peat smoke increased AGP levels relative to low peat smoke and air ($p < 0.05$) at 2 h. AGP levels in the air group at 6 h were greater than the levels in both endpoints in the corresponding group at 0 h. Increases in circulating AGP have been previously demonstrated after ozone exposure in rats (Bass et al. 2013). Because these acute phase proteins are likely originating from the liver (Blackburn 1994), it is plausible that AGP release was in part mediated by autonomic stimulation. There were little to no effects of exposure and/or gavage on complete blood count endpoints and other indicators of systemic injury and inflammation (data not shown).

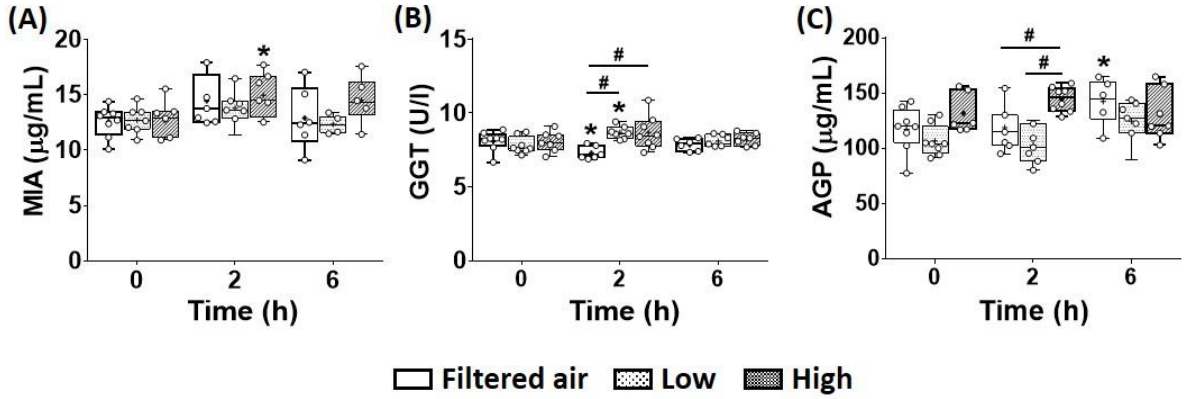

Figure 15. Postprandial changes in pulmonary and systemic indicators of inflammation and injury in peat smoke-exposed rats. (A) MIA (micro albumin), (B) GGT (gamma-glutamyl transferase), (C) AGP (alpha-1 acid glycoprotein). Data are reported using boxplots with significant changes in corresponding groups across time points indicated with * and significant changes compared to filtered air within a certain time point are indicated with #.

Peat smoke impacts on blood monocytes measured in un-gavaged rats at 0 h or 6 h after HF gavage are shown in Figure 16. Low peat smoke increased the percentage of monocytes that were classical monocytes relative to filtered air at 0 h and at 6 h (Figure 16A; $p < 0.05$). There were no effects of peat smoke exposure on the percentage of monocytes that were CD11 b/c monocytes at 0 h (Figure 16B). Low peat smoke at 6 h, however, had elevated levels of CD11 b/c monocytes compared to air and high peat smoke at 6 h and relative to the corresponding group at 0 h. This effect was not evident in similarly exposed un-gavaged rats at 0 h. CD11 b/c monocytes are pro-inflammatory and pro-atherogenic and have been previously linked to accelerated vascular wall remodeling in a mouse model of vascular wall injury (Martinez et al. 2015). It is possible that classical monocytes converted to CD11 b/c expressing monocytes after gavage, since exposure to low peat alone caused an increase in classical monocytes in un-gavaged rats. Classical monocytes are linked to inflammatory responses (Kratofil et al. 2017) as evidenced by increases in these cells after pulmonary exposure to lipopolysaccharide in rats (Barnett-Vanes et al. 2016). These findings collectively indicate that HF challenge after even short-term air pollution exposure causes a transient shift towards a pro-inflammatory phenotype that when extrapolated over a life time of exposure and consumption of a HF diet may set the stage for initiation and/or progression of

cardiovascular diseases including atherosclerosis.

Non-Linear Dose-Response Relationship between Peak Smoke and Health Effects

The biological responses to low and high peat smoke exposure point to an absence of a traditional concentration-response pattern, wherein the magnitude of responses increases with higher exposure concentration/dose. In fact, unique low dose effects have been previously reported including the elicitation of a lung cytokine expression pattern with repeated low dose diesel exhaust exposure that was absent at higher doses in a mouse model (Saito et al. 2002). We previously reported elicitation of electrocardiographic alterations (i.e. ST depression) with a single exposure to diesel exhaust gases that was not evident at the higher concentration (Lamb et al. 2012). Furthermore, we demonstrated that exposure to low concentrations of residual oil fly ash (Farraj et al. 2011) or diesel exhaust (Hazari et al. 2011) were as potent in increasing sensitivity to cardiac arrhythmogenic challenge as higher concentrations, while eliciting disparate electrocardiographic and autonomic effects. The precise phenomena driving these effects are unclear, but reflect the complexity inherent in particle-gas mixtures, the health effects of which are likely determined by the interplay of physicochemical and biological mechanisms at each exposure dose. Although the low and high peat smoke had similar organic carbon content, pointing to potentially comparable chemical composition, low peat had smaller particle size, which may have influenced the response pattern observed. Compared to larger particles, smaller particles have a greater capacity for deep lung penetration and likewise elicitation of pulmonary and systemic inflammatory responses and injury (Brook et al. 2010).

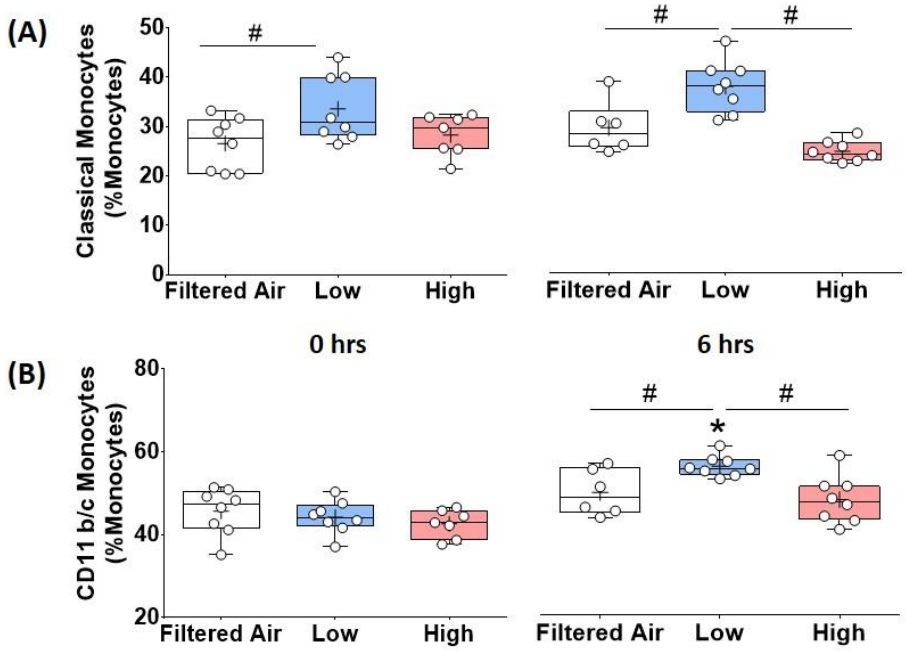

Figure 16. Postprandial changes in circulating monocyte phenotype in peat smoke-exposed rats. Data are reported using boxplots with significant changes in corresponding groups across time points indicated with * and significant changes compared to filtered air within a certain time point are indicated with #.

Conclusions and Implications for Management/Policy and Future Research

We have developed a novel combustion and smoke-collection system that can be used for chemical/toxicological analyses of biomass smoke under precise combustion conditions and whose data can be used to understand the potential health effects from exposures to various biomass combustions. We have also demonstrated that the combustion system operated with an active feedback controller can successfully supply stable biomass smoke concentrations (e.g., PM and CO) under various combustion conditions and maintain target set values. This allows for the accurate delivery of specific biomass smoke concentrations to the inhalation chamber, and to accurately estimate biomass smoke PM doses delivered to the lungs.

Both the chemical and toxicological data illustrate the distinctive contribution of vertical versus horizontal or wood versus non-wood components of wildlands to the adverse biological effects of wildland fires, suggesting that emissions from fires in regions rich in those type of fuels may induce greater health effects than those from fires of similar magnitude with other types of biomass. Overall, our findings demonstrate that the lung toxicity and mutagenic potencies of biomass smoke emissions on a mass basis were greater from flaming than smoldering phases for a variety of biomass fuels. Furthermore, biomass smoke exposure sensitized the body to non-specific stressors of the cardiovascular system like a high fat challenge, resulting in exaggerated systemic and pulmonary injury. Such data should provide guidance on the protection from inhalation to wildland fire smoke for firefighter and public health responses to wildland fires, whose scale and severity are increasing worldwide.

The primary goal of this research was to aid in the specificity of regional public health alerts, and to provide strategies for chemo-prevention in firefighters as well as people living in communities near or downwind of wildland fires. However, it is also well recognized that wildfire smoke (specifically, gases and particles) can be photochemically transformed (or aged) in the atmosphere and transported into populated urban areas that are hundreds of miles away from the fires. Thus, it is necessary to investigate health effects of exposures to not only fresh wildfire smoke but also aged smoke. Future research should address 1) a more in-depth analysis of the toxicity of both fresh and aged wildland fire smoke, 2) information on how atmospheric aging and transportation of wildfire smoke causes potential health effects in urban areas and if this is more or less potent than traditional urban air pollutants such as vehicular exhaust, and 3) a data base for extrapolating to real-world wildfire smoke exposure situations.

Literature Cited

Abatzoglou JT, Williams AP (2016) Impact of anthropogenic climate change on wildfire across western US forests Proceedings of the National Academy of Sciences of the United States of America 113:11770-11775

Adetona O et al. (2016) Review of the health effects of wildland fire smoke on wildland firefighters and the public Inhalation toxicology 28:95-139

Asgharian B et al. (2014) Computational modeling of nanoscale and microscale particle deposition, retention and dosimetry in the mouse respiratory tract Inhal Toxicol 26:829-842

Asita AO et al. (1991) Mutagenicity of wood smoke condensates in the Salmonella/microsome assay Mutat Res 264:7-14

Barnett-Vanes A, Sharrock A, Birrell MA, Rankin S (2016) A Single 9-Colour Flow Cytometric Method to Characterise Major Leukocyte Populations in the Rat: Validation in a Model of LPS-Induced Pulmonary Inflammation PloS one 11:e0142520

Bass V et al. (2013) Ozone induces glucose intolerance and systemic metabolic effects in young and aged Brown Norway rats Toxicology and applied pharmacology 273:551-560

Blackburn WD, Jr. (1994) Validity of acute phase proteins as markers of disease activity The Journal of rheumatology Supplement 42:9-13
Bolling AK, Pagels J, Yttri KE, Barregard L, Sallsten G, Schwarze PE, Boman C (2009) Health effects of residential wood smoke particles: the importance of combustion conditions and physicochemical particle properties Particle and fibre toxicology 6:29
Bolling AK et al. (2012) Wood smoke particles from different combustion phases induce similar pro-inflammatory effects in a co-culture of monocyte and pneumocyte cell lines Particle and fibre toxicology 9:45
Brook RD et al. (2010) Particulate matter air pollution and cardiovascular disease: An update to the scientific statement from the American Heart Association Circulation 121:2331-2378
Burling IR et al. (2010) Laboratory measurements of trace gas emissions from biomass burning of fuel types from the southeastern and southwestern United States Atmos Chem Phys 10:11115-11130
Canova C et al. (2010) Carbon monoxide pollution is associated with decreased lung function in asthmatic adults Eur Respir J 35:266-272
Cascio WE (2018) Wildland fire smoke and human health Sci Total Environ 624:586-595
de Muñiz GIB, Lengowski EC, Nisgoski S, de Magalhães WLE, de Oliveira VT, Hansel F (2014) Characterization of Pinus spp needles and evaluation of their potential use for energy Cerne 20:248-250
De Vleeschouwer F, Chambers FM, Swindles GT (2010) Coring and sub-sampling of peatlands for palaeoenvironmental research Mires Peat 7:1-10
DeMarini DM, Lemieux PM, Ryan JV, Brooks LR, Williams RW (1994) Mutagenicity and chemical analysis of emissions from the open burning of scrap rubber tires Environmental science & technology 28:136-141
Dogan A et al. (2011) Acute effects of passive smoking on left ventricular systolic and diastolic function in healthy volunteers Journal of the American Society of Echocardiography : official publication of the American Society of Echocardiography 24:185-191
Dolinay T, Szilasi M, Liu M, Choi AM (2004) Inhaled carbon monoxide confers antiinflammatory effects against ventilator-induced lung injury Am J Respir Crit Care Med 170:613-620
Real Time Ambient Air Quality Data (2018) Dehli Pollution Control Committee (DPCC).
Driscoll KE, Costa DL, Hatch G, Henderson R, Oberdorster G, Salem H, Schlesinger RB (2000) Intratracheal instillation as an exposure technique for the evaluation of respiratory tract toxicity: uses and limitations Toxicological sciences : an official journal of the Society of Toxicology 55:24-35
Fang T, Guo H, Zeng L, Verma V, Nenes A, Weber RJ (2017) Highly Acidic Ambient Particles, Soluble Metals, and Oxidative Potential: A Link between Sulfate and Aerosol Toxicity Environmental science & technology 51:2611-2620
Farraj AK et al. (2011) ST depression, arrhythmia, vagal dominance, and reduced cardiac micro-RNA in particulate-exposed rats American journal of respiratory cell and molecular biology 44:185-196
Foresti R, Bani-Hani MG, Motterlini R (2008) Use of carbon monoxide as a therapeutic agent: promises and challenges Intensive Care Med 34:649-658
Foster WM, Walters DM, Longphre M, Macri K, Miller LM (2001) Methodology for the measurement of mucociliary function in the mouse by scintigraphy J Appl Physiol 90:1111-1117
Frey AK et al. (2009) Chemical composition and mass size distribution of fine particulate matter emitted by a small masonry heater Boreal Env Res 14:255-271
Gavett SH, Madison SL, Dreher KL, Winsett DW, McGee JK, Costa DL (1997) Metal and sulfate composition of residual oil fly ash determines airway hyperreactivity and lung injury in rats Environmental research 72:162-172
Geron C, Hays M (2013) Air emissions from organic soil burning on the coastal plain of North Carolina Atmos Environ 64:192-199
Gibbs-Flournoy EA et al. (2018) Differential exposure and acute health impacts of inhaled solid-fuel emissions from rudimentary and advanced cookstoves in female CD-1 mice Environ Res 161:35-48
Gibson DG, Francis DP (2003) Clinical assessment of left ventricular diastolic function Heart (British

Cardiac Society) 89:231-238
Gilman JB et al. (2015) Biomass burning emissions and potential air quality impacts of volatile organic compounds and other trace gases from fuels common in the US Atmos Chem Phys 15:13915-13938
Goebel U et al. (2008) Carbon monoxide inhalation reduces pulmonary inflammatory response during cardiopulmonary bypass in pigs Anesthesiology 108:1025-1036
Goldberg DM (1980) Structural, functional, and clinical aspects of gamma-glutamyltransferase CRC critical reviews in clinical laboratory sciences 12:1-58
Greenberg JP, Friedli H, Guenther AB, Hanson D, Harley P, Karl T (2006) Volatile organic emissions from the distillation and pyrolysis of vegetation Atmos Chem Phys 6:81-91
Gu L, Pandey V, Geenen DL, Chowdhury SA, Piano MR (2008) Cigarette smoke-induced left ventricular remodelling is associated with activation of mitogen-activated protein kinases European journal of heart failure 10:1057-1064
Happo MS et al. (2013) Pulmonary inflammation and tissue damage in the mouse lung after exposure to PM samples from biomass heating appliances of old and modern technologies The Science of the total environment 443:256-266
Hazari MS, Haykal-Coates N, Winsett DW, Krantz QT, King C, Costa DL, Farraj AK (2011) TRPA1 and sympathetic activation contribute to increased risk of triggered cardiac arrhythmias in hypertensive rats exposed to diesel exhaust Environmental health perspectives 119:951-957
IARC (2010) Household use of solid fuels and high-temperature frying. In: IARC Monographs on the Evaluation of Carcinogenic Risks to Humans, vol 95. International Agency for Research on Cancer (IARC) Working Group, Lyon, France,
Jaffe DA, Wigder NL (2012) Ozone production from wildfires: A critical review Atmos Environ 51:1-10
Jean J-C, Liu Y, Joyce-Brady M (2003) The importance of gamma-glutamyl transferase in lung glutathione homeostasis and antioxidant defense BioFactors 17:161-173
Johnston FH et al. (2012) Estimated global mortality attributable to smoke from landscape fires Environmental health perspectives 120:695-701
Kato M et al. (2004) Urinary biomarkers in charcoal workers exposed to wood smoke in Bahia State, Brazil Cancer epidemiology, biomarkers & prevention : a publication of the American Association for Cancer Research, cosponsored by the American Society of Preventive Oncology 13:1005-1012
Kellison RC, Lea R, Marsh P (2013) Introduction of eucalyptus spp. into the United States with special emphasis on the southern United States Int J Forest Res 2013:9
Kim YH et al. (2014) Cardiopulmonary toxicity of peat wildfire particulate matter and the predictive utility of precision cut lung slices Particle and fibre toxicology 11:29
Kim YH et al. (2018) Mutagenicity and Lung Toxicity of Smoldering vs. Flaming Emissions from Various Biomass Fuels: Implications for Health Effects from Wildland Fires Environ Health Perspect 126:017011
Kleeman MJ, Schauer JJ, Cass GR (1999) Size and composition distribution of fine particulate matter emitted from wood burning, meat charbroiling, and cigarettes Environ Sci Technol 33:3516-3523
Kleinman MT, Mautz WJ (1991) The effects of exercise on dose and dose distribution of inhaled automotive pollutants Res Rep Health Eff Inst:1-40; discussion 41-50
Klimisch H-J, Hollander HWM, Thyssen J (1980) Generation of constant concentrations of thermal decomposition products in inhalation chambers. A comparative study with a method according to DIN 53436. I. Measurement of carbon monoxide and carbon dioxide in inhalation chambers J Combust Toxicol 7:243-256
Kratofil RM, Kubes P, Deniset JF (2017) Monocyte Conversion During Inflammation and Injury Arteriosclerosis, thrombosis, and vascular biology 37:35-42
Lacaux JP, Delmas R, Jambert C, Kuhlbusch TAJ (1996) NOx emissions from African savanna fires J Geophys Res 101:23585-23595
Lamb CM et al. (2012) Divergent electrocardiographic responses to whole and particle-free diesel exhaust inhalation in spontaneously hypertensive rats Toxicological sciences : an official journal of the Society of Toxicology 125:558-568

Lawless JF (1987) Negative binomial and mixed Poisson regression Can J Stat 15:209-225
Linak WP, Ryan JV, Perry E, Williams RW, DeMarini DM (1989) Chemical and biological characterization of products of incomplete combustion from the simulated field burning of agricultural plastic Japca 39:836-846
Liu JC, Pereira G, Uhl SA, Bravo MA, Bell ML (2015) A systematic review of the physical health impacts from non-occupational exposure to wildfire smoke Environ Res 136:120-132
Long AS et al. (2014) Human urinary mutagenicity after wood smoke exposure during traditional temazcal use Mutagenesis 29:367-377
Maron DM, Ames BN (1983) Revised methods for the Salmonella mutagenicity test Mutation research 113:173-215
Martin BL et al. (2018) Acute peat smoke inhalation sensitizes rats to the postprandial cardiometabolic effects of a high fat oral load The Science of the total environment 643:378-391
Martinez L, Gomez C, Vazquez-Padron RI (2015) Age-related changes in monocytes exacerbate neointimal hyperplasia after vascular injury Oncotarget 6:17054-17064
McDonald JD, Zielinska B, Fujita EM, Sagebiel JC, Chow JC, Watson JG (2000) Fine particle and gaseous emission rates from residential wood combustion Environmental science & technology 34:2080-2091
McDow SR, Huntzicker JJ (1990) Vapor adsorption artifact in the sampling of organic aerosol: Face velocity effects Atmos Environ Part A 24:2563-2571
McMahon CK, Tsoukalas SN (1978) Polynuclear aromatic hydrocarbons in forest fire smoke. In: Jones PW, Freudenthal RI (eds) Carcinogenesis, Vol. 3: Polynuclear Aromatic Hydrocarbons, vol 3. Raven Press, New York, pp 61-73
McMeeking GR et al. (2009) Emissions of trace gases and aerosols during the open combustion of biomass in the laboratory J Geophys Res-Atmos 114:D19210
Morvay ZK, Gvozdenac DD (2008) Part III: Toolbox – Fundamentals for analysis and calculation of energy and environmental performance. Applied Industrial Energy and Enviromental Management. John Wiley & Sons, West Sussex, United Kingdom
Mutlu E et al. (2016) Mutagenicity and pollutant emission factors of solid-fuel cookstoves: comparison with other combustion sources Environmental health perspectives 124:974-982
Mutlu E et al. (2015) Health effects of soy-biodiesel emissions: bioassay-directed fractionation for mutagenicity Inhalation toxicology 27:597-612
Nielson RW, Dobie J, Wright DM (1985) Conversion factors for the forest product industry in western Canada. Western Laboratory, Forintek Canada Corp.
Otterbein LE et al. (2000) Carbon monoxide has anti-inflammatory effects involving the mitogen-activated protein kinase pathway Nat Med 6:422-428
Peter JI (1979) How to estimate recoverable heat energy in wood or bark fuels. Forest Products Laboratory, U.S. Gevernment Printing Office
Pimenta AS, Bayona JM, García MT, Solanas AM (2000) Evaluation of acute toxicity and genotoxicity of liquid products from pyrolysis of eucalyptus grandis wood Arch Environ Contam Toxicol 38:169-175
Rau JA (1989) Composition and size distribution of residential wood smoke particles Aerosol Sci Technol 10:181-192
Reid CE, Brauer M, Johnston FH, Jerrett M, Balmes JR, Elliott CT (2016) Critical review of health impacts of wildfire smoke exposure Environ Health Perspect 124:1334-1343
Reid JS, Hobbs PV (1998) Physical and optical properties of young smoke from individual biomass fires in Brazil J Geophys Res Atmos 103:32013-32030
Reid JS, Koppmann R, Eck TF, Eleuterio DP (2005) A review of biomass burning emissions part II: intensive physical properties of biomass burning particles Atmos Chem Phys 5:799-825 d
Reisen F, Duran SM, Flannigan M, Elliott C, Rideout K (2015) Wildfire smoke and public health risk Int J Wildland Fire 24:1029-1044
Reiss R, Anderson EL, Cross CE, Hidy G, Hoel D, McClellan R, Moolgavkar S (2007) Evidence of health impacts of sulfate-and nitrate-containing particles in ambient air Inhalation toxicology 19:419-449
Rose JJ, Wang L, Xu Q, McTiernan CF, Shiva S, Tejero J, Gladwin MT (2017) Carbon monoxide

poisoning: pathogenesis, management, and future directions of therapy Am J Respir Crit Care Med 195:596-606
Rosenkranz SK, Townsend DK, Steffens SE, Harms CA (2010) Effects of a high-fat meal on pulmonary function in healthy subjects European journal of applied physiology 109:499-506
Saito Y, Azuma A, Kudo S, Takizawa H, Sugawara I (2002) Long-term inhalation of diesel exhaust affects cytokine expression in murine lung tissues: comparison between low- and high-dose diesel exhaust exposure Experimental lung research 28:493-506
Swiston JR, Davidson W, Attridge S, Li GT, Brauer M, van Eeden SF (2008) Wood smoke exposure induces a pulmonary and systemic inflammatory response in firefighters The European respiratory journal 32:129-138
UNEP (1999) Wildland Fires and the Environment: a Global Synthesis.
Urbanski S (2014) Wildland fire emissions, carbon, and climate: emission factors Forest Ecol Manage 317:51-60
Veranth JM et al. (2006) Correlation of in vitro cytokine responses with the chemical composition of soil-derived particulate matter Environmental health perspectives 114:341-349
Ward DE, Radke LF (1993) Emissions measurements from vegetation fires: A comparative evaluation of methods and results. In: Crutzen PJ, Goldammer JG (eds) Fire in the Environment: The Ecological, Atmospheric, and Climatic Importance of Vegetation Fires. John Wiley & Sons, Chichester, England,
Watts RR et al. (1992) Development of source testing, analytical, and mutagenicity bioassay procedures for evaluating emissions from municipal and hospital waste combustors Environmental health perspectives 98:227-234
Werley MS, Lee KM, Lemus-Olalde R (2009) Toxicological responses in SW mice exposed to inhaled pyrolysates of polymer/tobacco mixtures and blended tobacco Inhalation toxicology 21:1186-1199
Westerling AL, Hidalgo HG, Cayan DR, Swetnam TW (2006) Warming and earlier spring increase western U.S. forest wildfire activity Science (New York, NY) 313:940-943
Wilson MR, O'Dea KP, Dorr AD, Yamamoto H, Goddard ME, Takata M (2010) Efficacy and safety of inhaled carbon monoxide during pulmonary inflammation in mice PloS one 5:e11565
Wong BA (2007) Inhalation exposure systems: design, methods and operation Toxicol Pathol 35:3-14
Youssouf H et al. (2014) Non-accidental health impacts of wildfire smoke Int J Environ Res Public Health 11:11772-11804

Appendix A: Contract Information for Key Project Personnel

M. Ian Gilmour, Ph.D., DABT, Principal Investigator
Environmental Public Health Division
National Health and Environmental Effects Research Laboratory
U.S. Environmental Protection Agency
109 TW Alexander Dr.
Research Triangle Park, NC 27711
gilmour.ian@epa.gov

Mark Higuchi, Ph.D., Co-Principal Investigator
Environmental Public Health Division
National Health and Environmental Effects Research Laboratory
U.S. Environmental Protection Agency
109 TW Alexander Dr.
Research Triangle Park, NC 27711
higuchi.mark@epa.gov

Michael D. Hays, Ph.D., Co-Principal Investigator
Air and Energy Management Division
National Risk Management Research Laboratory
U.S. Environmental Protection Agency
109 TW Alexander Dr.
Research Triangle Park, NC 27711
hays.michael@epa.gov

Aimen Farraj, Ph.D., DABT, Co-Principal Investigator
Environmental Public Health Division
National Health and Environmental Effects Research Laboratory
U.S. Environmental Protection Agency
109 TW Alexander Dr.
Research Triangle Park, NC 27711
farraj.aimen@epa.gov

David M. DeMarini, Ph.D., Co-Principal Investigator
Integrated Systems Toxicology Division
National Health and Environmental Effects Research Laboratory
U.S. Environmental Protection Agency
109 TW Alexander Dr.
Research Triangle Park, NC 27711
demarini.david@epa.gov

Appendix B. List of Completed/Planned Scientific/Technical Publications/Science Delivery Products

1. Articles in peer-reviewed journals

L.C. Thompson, Y.H. Kim, B.L. Martin, A.D. Ledbetter, M.S. Hazari, M.I. Gilmour, A.K. Farraj, Pulmonary exposure to peat smoke extracts in rats decreases expiratory time and increases left heart end systolic volume, Inhalation Toxicology, 2018, in press.

Y.H. Kim, S.H. Warren, Q.T. Krantz, C. King, R. Jaskot, W.T. Preston, B.J. George, M.D. Hays, M.S. Landis, M. Higuchi, D.M. DeMarini, M.I. Gilmour, Mutagenicity and lung toxicity of smoldering versus flaming emissions from various biomass fuels: Implications for health effects from wildland fires, Environmental Health Perspectives, 2018, 126:017011.

B.L. Martin, L.C. Thompson, Y.H. Kim, W. Williams, S.J. Snow, M.C. Schladweiler, P. Phillips, C. King, J. Richards, N. Haykal-Coates, M. Higuchi, M.I. Gilmour, U.P. Kodavanti, M.S. Hazari, A.K. Farraj, Acute peat smoke inhalation sensitizes rats to the postprandial cardiometabolic effects of a high fat oral load, Science of the Total Environment, 2018, 643, 378-391

M.I. Gilmour, Y.H. Kim, M. Hays, Comparative chemistry and toxicity of diesel and biomass combustion emissions, Analytical and Bioanalytical Chemistry, 2015, 407, 5869-5875.

Y.H. Kim, C. King, Q.T. Krantz, I.J. George, M. McGee, J. McGee, L. Copeland, M.D. Hays, M.S. Landis, M. Higuchi, D.M. S.H. Gavett, M.I. Gilmour, The role of fuel types and combustion phases on the toxicity of biomass smoke following inhalation exposure in mice, submitted to Archives of Toxicology, 2018.

2. Conference or symposium abstracts

Y.H. Kim, M.I. Gilmour, Comparison of precision cut lung slices and whole lungs in particle-induced inflammation, Society of Toxicology Annual Meeting, Mar. 10-14, 2019, Baltimore, MD, U.S.A.

B.L. Martin, L.C. Thompson, Y.H. Kim, S.J. Snow, M.C. Schladweiler, P. Philips, C. King, J. Richards, N. Haykal-Coates, M.I. Gilmour, U.P. Kodavanti, M.S. Hazari, A.K. Farraj, Acute eucalyptus smoke inhalation sensitizes rats to the postprandial cardiometabolic effects of a high carbohydrate oral load, Society of Toxicology Annual Meeting, Mar. 10-14, 2019, Baltimore, MD, U.S.A.

A.K Farraj, B.L. Martin, L.C. Thompson, Y.H. Kim, S.J. Snow, M.C. Schladweiler, N. Haykal-Coates, I. George, M.I. Gilmour, U.P. Kodavanti, M.S. Hazari, Baroreflex sensitivity and cardiovascular responses to acute peat smoke inhalation in rats, Society of Toxicology Annual Meeting, Mar. 10-14, 2019, Baltimore, MD, U.S.A.

M.M. Hargrove, Y.H. Kim, C. King, M.I. Gilmour, S.H. Gavett, Greater respiratory effects of acute biomass smoke inhalation in mice compared with episodic exposures, Society of Toxicology Annual Meeting, Mar. 10-14, 2019, Baltimore, MD, U.S.A.

W.K. Martin, S. Padilla, Y.H. Kim, M.D. Hays, D.L. Hunter, M.S. Hazari, M.I. Gilmour, A.K. Farraj, Zebrafish locomotor response to biomass emissions are influenced by fuel type, burn conditions and byproduct composition, Society of Toxicology Annual Meeting, Mar. 10-14, 2019, Baltimore, MD, U.S.A.

M. Harmon, Y.H. Kim, C. King, B. Martin, N. Coates, I.M. Gilmour, A.K. Farraj, M.S. Hazari, The effect of enriched vs. inadequate housing conditions on biomass smoke-induced cardiovascular dysfunction in mice, North Carolina Society of Toxicology Fall Meeting, Oct. 15, 2018, NIEHS, Research Triangle Park, NC, U.S.A.

Y.H. Kim, C. King, Q.T. Krantz, I.J. George, M.M. Hargrove, J. McGee, L. Copeland, M.D. Hays, M.S. Landis, M. Higuchi, S.H. Gavett, M.I. Gilmour, Comparison of aspiration and inhalation exposure methods for predicting pulmonary toxicity of biomass smoke, Fire Continuum Conference, May 21-24, 2018, Missoula, MT, U.S.A.

M. Jaoui, Y.H. Kim, C. King, M.I. Gilmour, M.S. Landis, Characterization of aerosol polar organic compounds of smoldering and flaming combustion of red oak, irish peat, and eucalyptus, Fire Continuum Conference, May 21-24, 2018, Missoula, MT, U.S.A.

Y.H. Kim, C. King, Q.T. Krantz, I.J. George, M.M. Hargrove, L. Copeland, M.D. Hays, M.S. Landis, M. Higuchi, S.H. Gavett, M.I. Gilmour, Concordance of pathophysiological responses in mice exposed to different biomass smoke conditions via aspiration and inhalation, Society of Toxicology Annual Meeting, Mar. 11-15, 2018, San Antonio, TX, U.S.A.

M.M. Hargrove, Y.H. Kim, C. King, C.E. Wood, L.B. Copeland, J.E. Richards, R. Jaskot, J.A. Dye, R. Grindstaff, M.I. Gilmour, S.H. Gavett, Smoldering eucalyptus and red oak smoke inhibit respiration in an allergic asthma mouse model, Society of Toxicology Annual Meeting, Mar. 11-15, 2018, San Antonio, TX, U.S.A.

S.H. Gavett, M.M. Hargrove, Y.H. Kim, C.E. Wood, L.B. Copeland, J.A. Dye, R. Jaskot, R.D. Grindstaff, M.I. Gilmour, Differential effects of wildfire biomass smoke inhalation on allergic inflammation in mice, Society of Toxicology Annual Meeting, Mar. 11-15, 2018, San Antonio, TX, U.S.A.

A.K. Farraj, B.L. Martin, L.C. Thompson, Y.H. Kim, C. King, S. Snow, M. Shladweiler, N. Haykal-Coates, I. George, M. Higuchi, M.I. Gilmour, U.P. Kodavanti, M.S. Hazari, Acute peat smoke inhalation increases blood pressure and cardiac arrhythmia risk in rats, Society of Toxicology Annual Meeting, Mar. 11-15, 2018, San Antonio, TX, U.S.A.

B.L. Martin, L.C. Thompson, Y.H. Kim, W. Williams, S.J. Snow, M.C. Schladweiler, P. Phillips, C. King, J. Richards, N. Haykal-Coates, M. Higuchi, M.I. Gilmour, U.P. Kodavanti, M.S. Hazari, A.K. Farraj, A high fat meal after peat smoke inhalation unmasks latent cardiopulmonary

responses, Society of Toxicology Annual Meeting, Mar. 11-15, 2018, San Antonio, TX, U.S.A.

Y.H. Kim, C. King, T. Krantz, I. George, M. McGee, L. Copeland, M. Hays, M. Landis, M. Higuchi, S. Gavett, M.I. Gilmour, Differential lung toxicity of biomass smoke from smoldering and flaming phases following acute inhalation exposure, American Association for Aerosol Research Annual Conference, Oct. 16-20, 2017, Raleigh, NC, U.S.A.

Y.H. Kim, S. Warren, T. Krantz, C. King, R. Jaskot, W.T. Preston, M. Hays, M. Landis, M. Higuchi, D. DeMarini, M.I. Gilmour, Differential mutagenicity and lung toxicity of smoldering versus flaming emissions from a variety of biomass fuels, Society of Toxicology Annual Meeting, Mar. 12-16, 2017, Baltimore, MD, U.S.A.

W.K. Martin, S. Padilla, Y.H. Kim, M.D. Hays, D.L. Hunter, M.S. Hazari, M.I. Gilmour, A.K. Farraj, Zebrafish locomotor responses predict irritant potential of smoke particulate matter from five biomass fuels, Society of Toxicology Annual Meeting, Mar. 12-16, 2017, Baltimore, MD, U.S.A.

L.C. Thompson, Y.H. Kim, B.L. Martin, A.D. Ledbetter, M.S. Hazari, M.I. Gilmour, A.K. Farraj, Peat biomass smoke particle exposure in rats decreases expiratory time and increases left heart end diastolic volume, Society of Toxicology Annual Meeting, Mar. 12-16, 2017, Baltimore, MD, U.S.A.

Y.H. Kim, S. Warren, T. Krantz, C. King, R. Jaskot, W.T. Preston, M. Hays, M. Landis, M. Higuchi, D. DeMarini, M.I. Gilmour, Mutagenicity and toxicity of biomass smoke are dependent on fuel type and combustion conditions, International Smoke Symposium, Nov. 14-17, 2016, Long Beach, CA, U.S.A.

Y.H. Kim, S. Warren, T. Krantz, C. King, R. Jaskot, M. Hays, M. Landis, M. Higuchi, D. DeMarini, M.I. Gilmour, Role of fuel and combustion conditions on mutagenicity and lung toxicity of wildfire emissions, VPS Symposium, May 4, 2016, Chapel Hill, NC, U.S.A.

Y.H. Kim, S. Warren, T. Krantz, C. King, R. Jaskot, M. Hays, M. Landis, M. Higuchi, D. DeMarini, M.I. Gilmour, Comparative study of emission factors and mutagenicity of red oak and peat smoke from smoldering and flaming combustion, International Fire Behavior and Fuels Conference, Apr. 11-15, 2016, Portland, OR, U.S.A.

Y.H. Kim, S. Warren, T. Krantz, C. King, R. Jaskot, M. Hays, M. Landis, M. Higuchi, D. DeMarini, M.I. Gilmour, Characterization and mutagenicity of smoke from smoldering and flaming combustion of peat and red oak biomass fuels, Society of Toxicology Annual Meeting, Mar. 13-17, 2016, New Orleans, LA, U.S.A.

M. Hays, M.I. Gilmour, Y.H. Kim, Experiments at the interface of carbon particle chemistry and toxicology, International Conference on Carbonaceous Particles in the Atmosphere, Aug. 10-13, 2015, Berkeley, CA, U.S.A.

3. Workshop materials and outcome reports

M.I. Gilmour (Workshop), Toxicological responses to biomass smoke under different combustion conditions, American Society of Public Health Annual meeting, Nov. 2018, San Diego, CA, U.S.A.

M.I. Gilmour (Webinar), Comparative toxicity of biomass smoke from different fuels and combustion conditions, Air Quality Research Subcommittee, National Oceanic and Aeronautical Agency, Apr. 2018.

M.I. Gilmour (Webinar), Relative toxicity of biomass smoke from different fuels and combustion conditions, Institute for Tribal Environmental Professionals, American Indian Air Quality Training Program, Jan. 2018.

M.I. Gilmour (Keynote Speaker), Regional and source specific comparisons of ambient particulate matter, Inhaled particles XII, Sep. 2017, Glasgow, Scotland.

M.I. Gilmour (Visiting Lecture), Role of fuel composition and combustion conditions on health impacts of emissions, Sep. 2017, Center for Inflammation Research, University of Edinburgh.

M.I. Gilmour (Keynote Speaker), Impact of air pollutants on the development of allergic lung disease, Ohio and Alleghany Regional Society of Toxicology, May 2016.

4. Presentations/webinars/other outreach/science delivery materials

EPA Training Video, Studying the Toxicity of Wildland Fire Smoke Using the Smoke Combustion System, May 2018: https://youtu.be/LlW532qWpBs

Environmental Health Perspectives (EHP) Science Selection, Flavors of Fires: Assessing the Relative Toxicity of Smoke from Different Types of Wildfires, Apr. 2018

EPA Blog, Simulating Wildland Fires in a Tube to Protect Public Health, May 2016

Role of Fuel and Combustion Conditions on Toxicity and Mutagenicity of Wildfire Emissions
EPA Exhibit Booth at the Fire Continuum Conference, May 2018
EPA Exhibit Booth at the American Association for Aerosol Research Annual Conference, Oct. 2017
EPA Exhibit Booth at the Society of Toxicology Annual Meeting, Mar. 2016

Appendix C. Metadata

All information for this project including experiment conditions, smoke sampling methods, sampling analysis, biological samples and physiological analysis are saved as Metadata_toxicity_biomass_smoke.xlsx and can be accessed from the US Forest Service Research Data Archive.